Mutational Studies on Catalytic Domain of D-stereospecific Amidohydrolase from *Streptomyces* sp. 82F2

放線菌由来 D 体特異的アミド加水分解酵素の触媒領域における変異解析

YASMEEN YOUSIF AHMED ELYAS

2018

DEDICATION

This thesis work is dedicated to:

To my husband, **Ayman**, who has been a constant source of support and encouragement during the challenges of graduate school life, to **Menatallah** my sweet daughter and also to **Ahmed** my lovely son.

This work also dedicated to my parents, **Yousif Elyas** and **Mhasien AbduElgader.**

Yasmeen,

ACKNOWLEDGMENT

*My profound gratitude goes to Almighty **Allah**, the omnipotent and omniscient, all the praise and glory are to Him alone for giving me the strengths, patience, knowledge, health, time, resources, opportunity and blessing to complete this study.*

*First, I would like to express my sincere gratitude to my advisor Prof. **Jiro Arima,** Department of Agricultural, Biological, and Environmental Sciences, Faculty of Agriculture, Tottori University, for his continuous support, valuable guidance, scholarly inputs and consistent encouragement I received throughout the research work. This feat was possible only because of the unconditional support provided by prof **Arima,** person with an amicable and positive disposition, prof **Arima** has always made himself available to clarify my doubts despite his busy schedules and I consider it as a great opportunity to do my doctoral programme under his guidance and to learn from his research expertise. Thank you, Prof **Arima**, for all your help and support.*

*My sincere gratitude goes to my Ph.D. co-supervisor Professor **Hiroyuki Azakami**, Department of Biological Chemistry, Faculty of Agriculture, Yamaguchi University, for extended discussions and valuable suggestions which have contributed greatly to the progress of this research.*

*Also, I would like to thank my former supervisor Dr. **Nuha Elkhatim** for her inspiration and advice during the first stage of my academic life.*

*My deepest thankfulness and appreciation offers to Dr. **Isam Ali Mohamed Ahmed**, Associate Professor Department of Food and Agricultural Sciences, King Saud University, who recommended and encouraged me to study in]apan, for his remarkable advice and help during the application process.*

*I am forever thankful to my colleagues at the Laboratory of Bio-Functional Chemistry, a former student and current for their friendship and support, and for creating a cordial working environment, especially, Mr. **Kazusa Miyatani**, Mr. **Yoshitaka Isoda**, Mr. **Taro Amano**.*

*I gratefully acknowledge the contributions of the **Ministry of Education, Science, Sports and Culture of Japan** for providing the financial support which removed financial concerns from my decision to embark on this journey.*

*My thanks and appreciation goes to the staff members of the **International Affairs Division Center, United Graduate School of Agricultural Sciences, Tottori University** for their unlimited help and support through my study and personal life.*

I would like to thank my colleagues, the academic, technical, and administrative staff of ***Khartoum University*** *for allowing me to complete my study in Japan.*

My thanks and appreciation goes to Dr. ***Yasir Serag Alnor*** *and Dr.* ***Nasreen Mohamed Kamal,*** *for their generous support and encouragement. I received a lot of help from them both in my research and personal life.*

My deepest love and appreciation goes to ***Ikuko Sekino,*** *Japanese language teacher for her patient, generosity, and emotional support, she has always been there for me in spite of her busy life.*

My deep and sincere gratitude to my family for their continuous and unparalleled love, help and support. I am grateful to my sisters ***Yousra*** *and* ***Yathrib*** *and my brother* ***Ahmed*** *for help and support. I am forever indebted to my parents, my mother* ***Mahasin Abdulgadir*** *and my father* ***Yousif Elyas*** *for their unconditional love, Patience, prayers and for giving me the opportunities and experiences that have made me who I am. They selflessly encouraged me to explore new directions in life and seek my own destiny. This journey would not have been possible if not for them, and I dedicate this milestone to them.*

Special thanks and love also goes to my second family, my father-in-law Mr. ***MohamedZain AbduElrahim*** *and my mother-in-law* ***Afaf Khidir*** *For their endless understanding, support, love, and prayers.*

Finally, I owe thanks to a very special person, my husband, ***Aiman*** *for his continued and unfailing love, support and understanding during my pursuit of a Ph.D. degree that made the completion of thesis possible. You were always around at times I thought that it is impossible to continue, you helped me to keep things in perspective. I greatly value his contribution and deeply appreciate his belief in me. I appreciate my kids, my little girl* ***Menaallah*** *and my little boy* ***Ahmed*** *for abiding my ignorance and the patience they showed during my study time. Words would never say how grateful I am to both of you. I consider myself the luckiest in the world to have such a lovely and caring family, standing beside me with their love and unconditional support.*

Yasmeen Yousif Elyas

2018

TABLE OF CONTENTS

LIST OF FIGURES

LIST OF TABLES

LIST OF ABBREVIATIONS

1,8-DAO	1,8-diaminooctane
Amp	Ampicillin
BSA	bovine serum albumin
D.W.	Distilled water
DAH	D-stereospecific amidohydrolase
DMSO	dimethyl sulfoxide
LB	Luria-Bertani
LC	liquid chromatography
MS	mass spectrometry
OEt	ethyl ester
OMe	methyl ester
PAGE	polyacrylamide gel electrophoresis
PCR	polymerase chain reaction
*p*NA	*p*-nitroaniline
SDS	sodium dodecyl sulfate
TEMED	*N*,*N*,*N*,*N*-tetramethylethylenediamine
Tris	Tris (hydroxymethyl) amino methane

Table 1: Amino acid and their abbreviations

Amino acid	3 letters	1 letter	Amino acid	3 letters	1 letter
Alanine	Ala	A	Leucine	Leu	L
Arginine	Arg	R	Lysine	Lys	K
Asparagine	Asn	N	Methionine	Met	M
Aspartate	Asp	D	Phenylalanine	Phe	F
Aspartate or Asparagine	Asx	B	Proline	Pro	P
Cysteine	Cys	C	Serine	Ser	S
Glutamate	Glu	E	Threonine	Thr	T
Glutamine	Gln	Q	Tryptophan	Trp	W
Glutamate or Glutamine	Glx	Z	Tyrosine	Tyr	Y
Glycine	Gly	G	Valine	Val	V
Histidine	His	H			
Isoleucine	Ile	I			

CHAPTER ONE

GENERAL INTRODUCTION

1.1 INTRODUCTION

Proteases likely arose at the earliest stages of protein evolution as simple destructive enzymes necessary for protein catabolism and the generation of amino acids in primitive organisms. For many years, studies on proteases focused on their original roles as blunt aggressors associated with protein demolition. However, the realization that, beyond these nonspecific degradative functions, proteases act as sharp scissors and catalyze highly specific reactions of proteolytic processing, producing new protein products, inaugurated a new era in protease research. Depends on their catalytic mechanisms, proteases are classified into six main classes: aspartic, threonine, metallo, cysteine, serine, and glutamic proteases, although glutamic proteases have not been found in mammals so far. Human cells produce at least 569 proteases including 194 metallo, 176 serine, 150 cysteine, 28 threonine and 21 aspartic proteases(López-otín and Matrisian 2007). Proteases cleave proteins from either the N-terminus or C-terminus (exopeptidases), or in the middle of a protein (endopeptidases). Much primary knowledge about the function of proteases stems from investigations of the digestive system and intracellular protein turnover. However, proteases are also considered as extremely important signaling molecules influenced by various biological events, such as apoptosis, blood coagulation, extracellular tissue remodeling and DNA replication(Rawlings and Barrett 1994; López-otín and Matrisian 2007).

Proteases have great medical and pharmaceutical importance due to their key role in biological processes and in the life-cycle of many pathogens. They are extensively applied

enzymes in several sectors of industry and biotechnology, furthermore, numerous research applications require their use, including production of Klenow fragments, peptide synthesis, digestion of unwanted proteins during nucleic acid purification, cell culturing and tissue dissociation, preparation of recombinant antibody fragments for research, diagnostics and therapy, exploration of the structure-function relationships by structural studies, removal of affinity tags from fusion proteins in recombinant protein techniques, peptide sequencing and proteolytic digestion of proteins in proteomics (Mótyán János András 2013).

Based on the catalytic mechanism and the presence of amino acid residue(s) at the active site the proteases can be grouped as aspartic proteases, cysteine proteases, glutamic proteases, metalloproteases, asparagine proteases, serine proteases, threonine proteases, and proteases with mixed or unknown catalytic mechanism. The current classification system further classifies the proteases into families based on sequence similarities, furthermore, homologous families are grouped into clans using a structure-based classification (Rawlings and Barrett 1993; Rawlings 2016). Classification and nomenclature of proteolytic enzymes, as well as a detailed description of individual proteases, is available in the MEROPS database (Rawlings et al. 2018).

1.2 SERINE PROTEASE

Almost one-third of all proteases can be classified as serine proteases, named for the nucleophilic Ser residue at the active site (Rawlings et al. 2016). Serine peptidases are the most widely studied group in biology, they can be found in eukaryotes, prokaryotes, archaea and viruses, interest in this family due to their widespread and distinctive role in a host of potential physiological and pathological process including digestion, hemostasis, apoptosis, signal transduction, and immune response (Hedstrom 2002a).

The catalytic action of serine peptidases depends on the interplay of a nucleophile, a general base, and an acid. In the first step of reaction a nucleophilic attack by the catalytic serine residue (active site Ser) on the carbonyl atom of the substrate resulting in a covalent acyl-enzyme intermediate and a new peptide amino terminus. a second nucleophilic attack, by a water molecule, leads to hydrolysis of the acyl-enzyme, releasing the new carboxyl group and restoring the catalytic Ser residue to its initial state. (Zakharova et al. 2009). In the presence of high concentrations of primary amines, which can not be achieved under physiological condition an amide bond is formed through nucleophilic attack by an amino group instead of a water molecule forms an amide bond (Fig. 1.1) (Bratovanova and Petkov 1987; John J. Perona and Charles S. Craik 1995). In this reaction, termed aminolysis the primary amine acts as an acyl acceptor. Because amino acids can act as acyl acceptors, the unnatural aminolysis reaction of serine peptidases has attracted attention as a method for synthesizing various peptides that cannot be produced under natural conditions. (Arima et al. 2016)

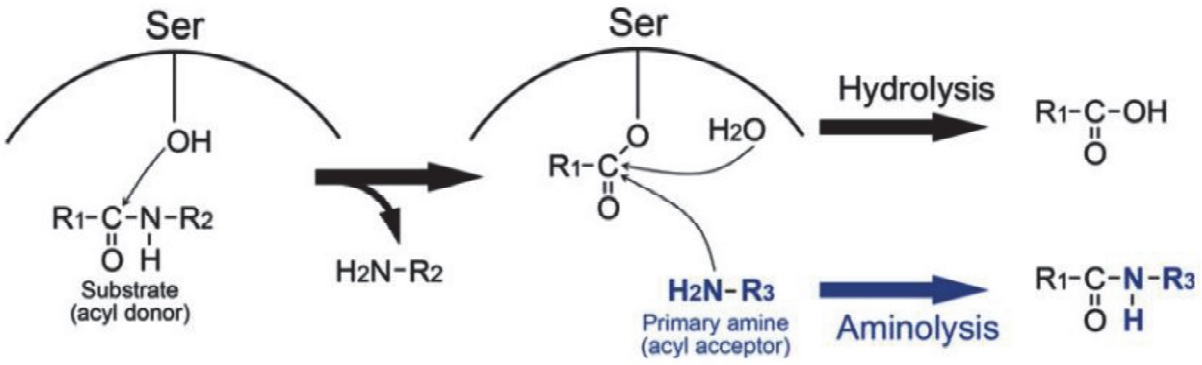

Fig. 1.1 Scheme of the hydrolysis and aminolysis reactions catalyzed by serine peptidases(Arima et al. 2016)

1.2.1 Classification of Serine Peptidase

The MEROPS protease classification system counts 16 super-families (as of 2013) each containing many families. Each superfamily uses the catalytic triad or dyad in a different protein fold and represents the convergent evolution of the catalytic mechanism. Families are grouped in a clan if there are indications, principally from tertiary structure comparisons, that they arise from a common ancestor. For every family and clan, there is an identifier that shows the catalytic type of the peptidases contained in the group. The identification marks are 'A' (aspartic), 'C' (cysteine), 'M' (metallo), 'S' (serine), 'P' (mixed catalytic type) and 'U' (unknown type) (Polgár 2005). Each clan, family, and the inhibitor is assigned to an identifier. For a clan, the identifier consists of two letters. The first indicates the catalytic type ('A' for aspartic peptidase, 'C' for cysteine peptidase, 'G' for glutamic peptidase, 'I' for inhibitors that are proteins, 'M' for metallopeptidase, 'P' for peptidases of mixed catalytic type, 'S' for serine peptidase, 'T' for threonine peptidase, 'N' for asparagine lyase, and 'U' for peptidases of unknown catalytic type. The second letter is assigned sequentially as each clan is identified. An example of a clan identifier is CA, which includes cysteine peptidases with a papain-like fold. For a family, the identifier consists of an initial letter, again corresponding to the catalytic type and a number. An example is C1, the family of papain-like cysteine peptidases (Rawlings et al. 2018).

Based on Barrett and Rawlings classification, the peptidases are divided into clans on the base of the catalytic mechanism and to families based on common ancestry (Rawlings 2009; Rawlings et al. 2016). Over 908300 peptidases protein sequences classified into 62 clans and 268 families (MEROPS 2018) (Rawlings et al. 2018). Serine peptidases represent almost one of third of all known proteolytic. More than 26000 serine peptidases have been classified into 13 clans and 82 families. The family name stems from the nucleophilic Ser in the enzyme

active site, which attacks the carbonyl moiety of the substrate peptide bond to form an acyl-enzyme intermediate. Nucleophilicity of the catalytic Ser is typically dependent on a catalytic triad of Asp, His, and Ser residues, commonly referred to as the charge relay system.

1.2.2 The catalytic mechanism of serine peptidase

The hallmark of serine peptidases is that they contain the so-called ‘‘classical’’ catalytic Ser/His/Asp triad. Although the classical serine proteases are the most widespread in nature, there exist a variety of ‘‘nonclassical’’ serine proteases where variations to the catalytic triad are observed. Such variations include the triads Ser/His/Glu, Ser/ His/His, and Ser/Glu/Asp, and include the dyads Ser/Lys and Ser/His. Other variations are seen with certain serine and threonine peptidases of the Ntn hydrolase superfamily that carry out catalysis with a single active site residue (Ekici et al. 2008). A summary of catalytic units in all serine peptidase families, primary specificity and the fold that harbors them are provided in Table 1.1.

Table 1.1. Known diversity of serine peptidase structure and catalytic mechanism.

Clan	Families	Representative member	Fold	Catalytic residues	#	Primary specificity	PDB
PA	12*	Trypsin	Greek-key β-barrels	His, Asp, Ser	195	A, D, F, G, K, Q, R, W, Y	1DPO
SB	2	Subtilisin, sedolisin	3-layer sandwich	Asp, His, Ser	221	F, W, Y	1SCN
SC	2	Prolyl oligopeptidase	α/β hydrolase	Ser, Asp, His	554	G, P	1QFS
SE	6	D-Ala–D-Ala carboxypeptidase	α-helical bundle	Ser, Lys	62	D-A	3PTE
SF	3	LexA peptidase	all β	Ser, Lys/His	119	A	1JHH
SH	2	Cytomegalovirus assemblin	α/β Barrel	His, Ser, His	132	A	1LAY
SJ	1	Lon peptidase	α+β	Ser, Lys	679	K, L, M, R, S	1RR9
SK	2	Clp peptidase	αβ	Ser, His, Asp	97	A	1TYF
SP	3	Nucleoporin	all β	His, Ser	na	F	1KO6
SQ	1	Aminopeptidase DmpA	4-layer sandwich	Ser	250	A, G, K, R	1B65
SR	1	Lactoferrin	3-layer sandwich	Lys, Ser	259	K, R	1LCT
SS	14	L,D-Carboxypeptidase	β-sheet+β-barrel	Ser, Glu, His	115	K	1ZRS
ST	5	Rhomboid	α-barrel	His, Ser	201	D, E	2IC8

A variety of catalytic units have arisen to assist the requisite nucleophilic Ser. #=residue acting as a nucleophile. *Seven additional families in clan PA of viral origin apply a nucleophilic Cys to mediate bond hydrolysis. (Page and Di Cera 2008)

The first well-characterized mechanism of action of serine peptidases was established primarily by the kinetic studies of chymotrypsin by Bender and his co-workers in the 1960s (Matthews et al. 1977). The X-ray data showed that the serine and histidine are the potent residues to catalysis and they are in proper position to function in the catalytic mechanism. As shown in figure (1.2) the OG of Ser195 and the NE2 of His57 are within hydrogen bonding distance. The other nitrogen atom (ND1) of the imidazole ring is hydrogen bonded to the carboxyl group of Asp102 so that the hydrogen bond is shielded from water by several amino acid residues. The geometric relation of Asp102, His57, and Ser195 led to the postulation that His57 serves for transferring the proton from Ser195 to Asp102 in a charge relay mechanism. However, a proton relay from the highly basic serine OH group to the acidic aspartate is chemically unlikely (Polgár and Bender 1969). It is a more reliable assumption that Asp102 may be involved in the stabilization of the ion-pair generated between the imidazolium ion and the negatively charged-tetrahedral intermediate, and that Asp102 may participate in the orientation of the correct tautomer of His57 relative to Ser195. Nuclear magnetic resonance (NMR) and neutron diffraction studies have then confirmed that it is the imidazole and not the aspartate that is protonated (Polgár 2005).

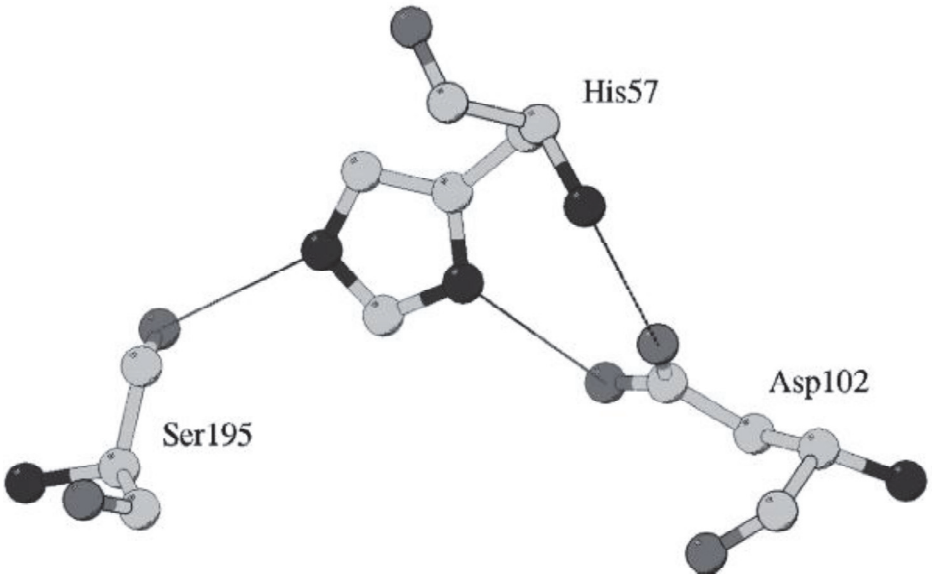

Fig. 1.2 The catalytic triad of chymotrypsin (PDB code 4CHA) (Polgár 2005)

All proteases must overcome three obstacles to hydrolyze a peptide bond: (a) amide bonds are very stable due to electron donation from the amide nitrogen to the carbonyl. For comparison, a simple bond, while a *p*-nitrophenyl ester is 300000× more alkyl ester is ~ 3000× more reactive than an amide reactive. Proteases usually activate an amide bond via the interaction of the carbonyl oxygen with a general acid, and may also distort the peptide bond to disrupt resonance stabilization; (b) water is a poor nucleophile; proteases always activate water, usually via a general base; and (c) amines are poor leaving groups; proteases protonate the amine prior to expulsion. Serine proteases perform these tasks very efficiently: the rates of peptide hydrolysis by serine proteases are ~10^{10}-fold greater than the uncatalyzed reactions. Obviously, these mechanisms of catalysis are not confined to peptide hydrolysis; serine proteases also readily hydrolyze other acyl compounds, including amides, anilides, esters, and thioesters. Figure 1.3 displays the generally accepted mechanism for chymotrypsin-like serine proteases. In the acylation half of the reaction, Ser195 attacks the carbonyl of the

peptide substrate, assisted by His57 acting as a general base, to yield a tetrahedral intermediate. The resulting His57-H^+ is stabilized by the hydrogen bond to Asp102. The oxyanion of the tetrahedral intermediate is stabilized by interaction with the main chain NHs of the oxyanion hole. The tetrahedral intermediate collapses with the expulsion of leaving the group, assisted by His57-H^+ acting as a general acid, to yield the acyl-enzyme intermediate. The deacylation half of the reaction essentially repeats the above sequence: water attacks the acyl-enzyme, assisted by His57, yielding a second tetrahedral intermediate. This intermediate collapses, expelling Ser195 and carboxylic acid product. The transition states of the acylation and deacylation reactions will resemble the high energy tetrahedral intermediates, and the terms "transition state" and "tetrahedral intermediate" are often used indiscriminately in the literature. It is worth noting that a web of hydrogen bonding interactions links the substrate binding sites to the catalytic triad. As the reaction proceeds, changes in bonding and charge at the scissile bond will propagate to more remote enzyme-substrate interactions, and vice versa. (Hedstrom 2002a)

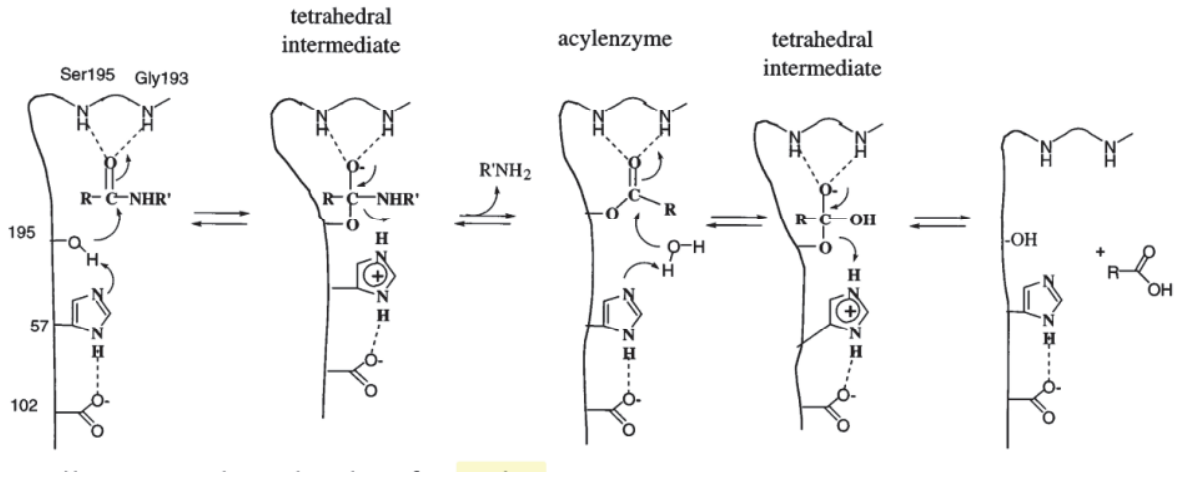

Fig. 1.3 The generally accepted mechanism for serine proteases. (Hedstrom 2002a)

1.3 D-STEREOSPECIFIC AMIDOHYDROLASE (DAH):

By Screening of 2000 soil isolates, D-stereospecific amidohydrolase (DAH) has been identified from the culture supernatant of *Streptomyces* sp. 82F2. The enzyme belongs to the S12 peptidase family with catalytic Ser / Lys dyad (Ser86 and Lys 89). DAH recognizes D-aminoacyl derivative as a substrate and amide bond is formed by aminolysis. The enzyme preferentially uses the D-aminoacyl derivative as the acyl donor and uses the L-amino acid and its derivative as the acyl acceptor to produce a dipeptide with the DL-configuration(Arima et al. 2011a, b). Therefore, DAH has been used to synthesize biologically active dipeptide such as cyclic dipeptide family 18 chitinase inhibitor, cyclo (D-Pro-L-Arg) in a one-step/one-pot reaction(Arima et al. 2011b).

Numbers of enzymes in the MEROPS peptidase database belonging to the S12 family, which have a catalytic Ser / Lys dyad, exhibit high aminolysis activity for various types of substrates such as amides esters and peptides (Kato et al. 1989, 1990; Pratt and Frère 2013). Up to date, five crystal structures of S12 family peptidases (including DAH) have been resolved: D-Ala-D-Ala carboxypeptidase B D, D-peptidase), class C b-lactamase, D-amino acid amidase (DAA) and D-stereospecific aminopeptidase D, D-peptidase, and D-stereospecific aminopeptidase catalyze peptide bond formation by their aminolysis activity (Lobkovskya et al. 1994; Kelly and Kuzin 1995; Bompard-Gilles et al. 2000; Okazaki et al. 2007; Arima et al. 2016). Based on these crystal structures, the structural factors responsible for the substrate specificities have been identified (Delmarcelle et al. 2005b).

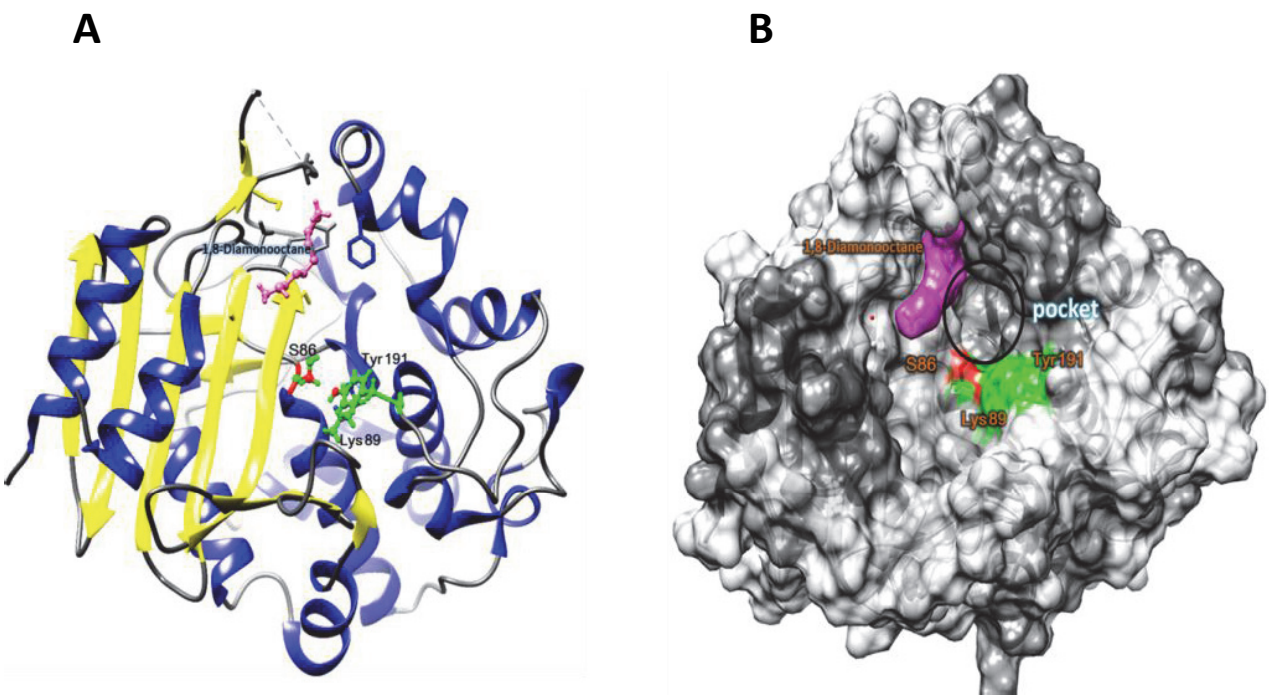

Fig. 1.4 Overall structure around the active site Ser86 of DAH. (A) The overall structure of DAH that interacts with 1,8-diaminooctane. a-Helices and b sheets are shown in red and yellow, respectively. (A) The overall structure of DAH that bounded with 1,8-diaminooctane. α-Helices and β sheets are shown in blue and yellow, respectively. The bound 1,8-diaminooctane and active site residues (Ser86, Lys89, and Tyr191) are shown as a purple and green ball and stick models, respectively. (B) Surface model of DAH. The active site Ser86 bound 1,8-diaminooctane and active site residues (Lys89 and Tyr191) are shown as red, purple and green, respectively.

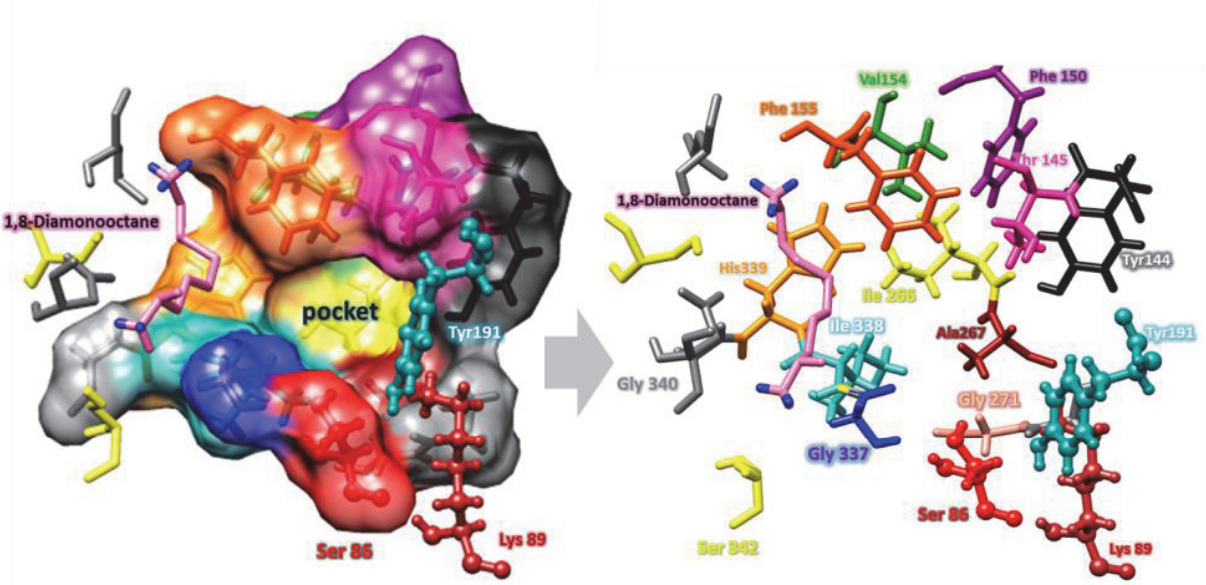

Fig. 1.5 The local structure of the active site pocket of DAH, and the residues composing the active site pocket. The active site residues (Ser86 and Lys89 and Tyr191) are shown as a ball and stick model according to the atom type. Other residues are shown as sticks colored according to the atom type.

1.3.1 Structure of the DAH:

Comparative analysis of DAH with homologous enzymes in same family S12 and crystallographic study provide insight into structural factors that affect the substrate specificity, stereoselectivity, and aminolysis activity. DAH can recognizes 1,8-diaminooctane and other amino acid compounds as acyl acceptor in aminolysis reaction, therefore, the crystal structure of DAH that binds 1,8-diaminooctane was determined at a resolution of 1.49 Å(Arima et al. 2016)

Figure (1.4) shows the overall structure of DAH, the enzyme consists of α-rich and ß-rich regions. The β-rich region is formed by residues 38–86 and 224–379, and consists of six main antiparallel b- strands flanked by four a-helices. The a-helix rich region (residues 87–223) includes another 11 α-helices Figure (1.4). The two motifs, Ser-x-x-Lys and Tyr-x-Asn, located at the N-terminal (Ser86–Lys89) and the internal region (Tyr191–Asn193) of DAH, respectively. Crystallographic analysis of the enzyme revealed that DAH possesses a large cavity that leads to the catalytic center. The side chains of Ser86 and Lys89 that create a catalytic Ser/Lys dyad in S12 family peptidases (Kelly and Kuzin 1995) were positioned at the center of the large cavity (Fig.1.4 A). hr191, which is close to the Ser/Lys dyad, acts as the general base to activate Ser as a nucleophile for the acyl donor during the acylation step and the water molecule during hydrolysis. In addition, there is a small pocket close to the catalytic center of Ser86, Ly89, and Tyr191 (Fig 1.4 B, and Fig 1.5). Structures comparison of family S12 enzymes, D, D-peptidase (PDB: 3PTE), D-amino acid amidase (PDB: 2EFX). Have revealed that DAH possess the largest cavity leading to catalytic center and large active site pocket beside DAA, therefore the large cavity and active site pocket allow the

substrate to enter, and accommodate the large side chain if acyl donor substrate (Fig 1.6) (Arima et al. 2016).

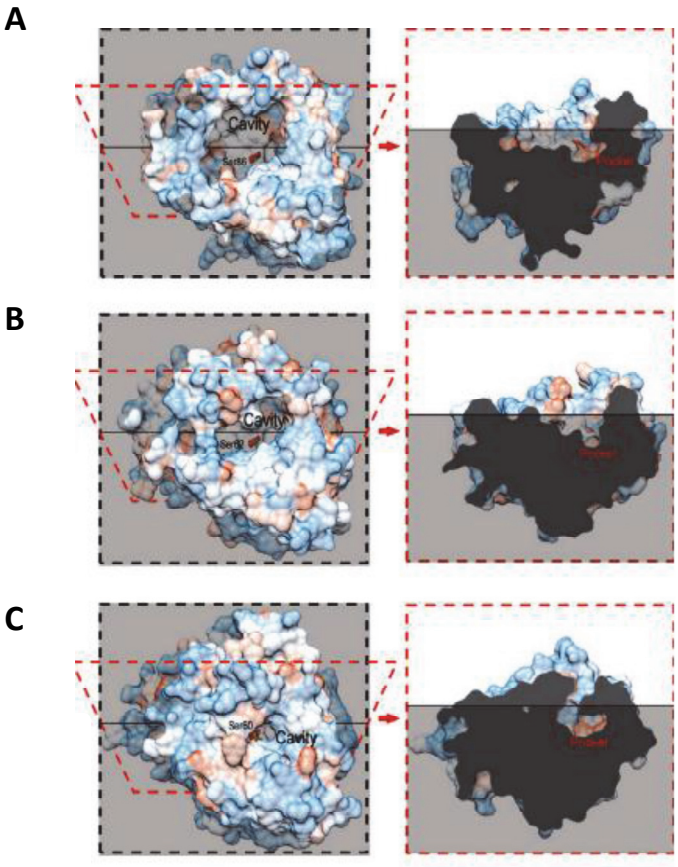

Fig. 1.6 Comparison of the cavity and pockets shapes of (A) DAH, (B) D, D-peptidase (Protein Data Bank code: 3PTE) and (C) DAA (Protein Data Bank code: 2EFX). The hydrophobic surfaces are also shown (left). Active site Ser residues of the enzymes are shown as ball and stick models colored according to the atom type. Corresponding cross-sectional views are shown on the right. The structures of respective enzymes are superimposed on the model of DAH, and then the cross-sectional view of respective enzymes with the same angle is created. The enzyme molecules are shown as hydrophobic surfaces. (Arima et al. 2016).

1.3.2 Mechanism of catalytic reaction of DAH

Several stereospecific peptidases that recognize an amide bond involving D-amino acid residues have been reported (Asano et al. 1989; Arima et al. 2010b). They are regarded as being associated mainly with the biosynthesis and remodeling of peptidoglycan. Among them, peptidases such as D-Ala–D-Ala carboxypeptidase B from *Streptomyces* sp. R61 (Kumar and Pratt 2005), D-aminopeptidase from *Ochrobactrum anthropi* (Kato et al. 1990), and D-peptidase from *Bacillus cereus*(Komeda and Asano 1999) have the function of an aminolysis reaction. The enzymes belonging to clan SE, the enzymes of the S11, S12, and S13 peptidase families, which are specialized for roles in bacterial cell wall metabolism.

The synthesis of diverse DL-configuration dipeptides in a one-pot reaction was demonstrated by using a function of the aminolysis reaction of a D-stereospecific amidohydrolase from *Streptomyces* sp.,(Arima et al. 2011b) a clan SE, S12 family peptidase categorized as a peptidase with D-stereospecificity. The enzyme was able to use various aminoacyl derivatives, including L-aminoacyl derivatives, as acyl donors and acceptors. Investigations of the specificity of the peptide synthetic activity revealed that the enzyme preferentially used D-aminoacyl derivatives as acyl donors. In contrast, L-amino acids and their derivatives were preferentially used as acyl acceptors. Consequently, the synthesized dipeptides had a DL-configuration when D- and L-aminoacyl derivatives were mixed in a one-pot reaction(Arima et al. 2011b).

DAH is also applicable for to synthesize biologically active dipeptides, such as cyclo(D-Pro–L-Arg), with the conversion rate of D- Pro-OBzl and L-Arg-OMe to cyclo(D-Pro–L-Arg) being greater than 65%. The cyclization of D-Pro–L-Arg-OMe occurred non-enzymatically (Fig. 1.7)(Arima et al. 2011b).

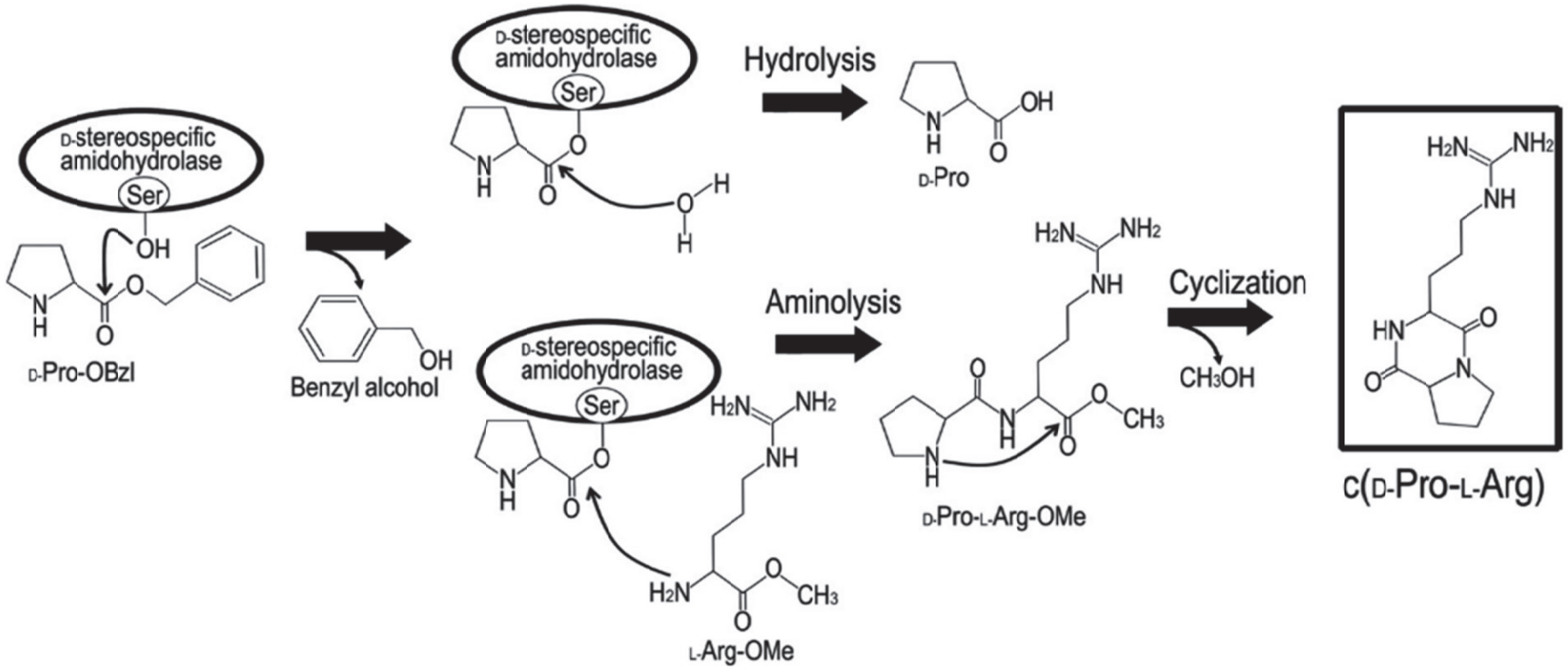

Fig. 1.7 Proposed mechanism for cyclo(D-Pro–L-Arg) [c(D-Pro–L-Arg)] production by a D-stereospecific amidohydrolase. (Arima et al. 2011b)

1.4 RESEARCH OBJECTIVES

According to the previously mentioned literature review, Serine proteases comprise nearly one-third of all known proteases identified to date and play crucial roles in a wide variety of cellular as well as extracellular functions, including the process of blood clotting, protein digestion, cell signaling, inflammation, fibrinolysis, fertilization, complement activation during immune responses and protein processing. (Rawlings and Barrett 1994; Page and Di Cera 2008) Owing to the expanding roles for serine proteases, there has been increasing interest in the identification, structural, and functional characterization of all members of the serine protease family of enzymes in humans and other organisms. Therefore, understanding the mechanism and structural factors affecting substrate recognition is important for the rational modification of enzymes and aimed at developing a convenient biocatalyst for peptide synthesis.

The assumption and concepts of the current study were to understand the structural implications of the D-Stereospecific amidohydrolase residues in and around the active site pocket and to investigate the effects of mutations of residues constituting the pocket on the catalysis and substrate specificity activity of DAH.

The Specific aims of the study were:

1- Mutational study on residues DAH active site pocket residues which are thought to involve in substrates recognition. We used site-directed mutagenesis to analyze the potential effects of alteration of eight residues to alanine aiming to expand the size of DAH pocket and investigated any changes in substrate recognition especially in the term of aminolysis reaction.

2- Assessing the effect of size/shape changes to the pocket on its substrate stereoselectivity and hydrophobic substrates recognition.

3- To assess the effect of the space filling of the active site pocket of DAH on catalytic activity to increase the aminolysis activity of the enzyme.

CHAPTER TWO

ACTIVE SITE POCKET OF STREPTOMYCES D-STEREOSPECIFIC AMIDOHYDROLASE HAS FUNCTIONAL ROLES IN AMINOLYSIS ACTIVITY

2.1 INTRODUCTION

Serine peptidases are widespread and abundant and play key roles in all living organisms. The enzymes are classified into 53 families (S1–S81 in the MEROPS peptidase database [http://merops.sanger.ac.uk/] (Rawlings et al. 2016; Rawlings 2016), and account for over 30% of all known proteolytic enzymes. The catalytic mechanism of all known serine peptidases involves a nucleophilic Ser residue that attacks the carbonyl moiety of the substrate peptide bond to form an acyl-enzyme intermediate. The substrate is an acyl donor. The intermediate is then hydrolyzed through nucleophilic attack by an activated water molecule. In the presence of high concentrations of primary amines, an amide bond is formed through nucleophilic attack by an amino group instead of a water molecule (Bratovanova and Petkov 1987; Arima et al. 2014). The primary amine acts as an acyl acceptor. This enzymatic aminolysis reaction has been used for the syntheses of various biologically active peptides, such as Kyotorphin (Arima et al. 2010a) infusion material (Yokozeki and Hara 2005) and carnosine (Heck et al. 2007; Arima et al. 2010b)

The nucleophilicity of the catalytic Ser of most serine peptidases is dependent on a catalytic triad of Asp, His, and Ser residues, commonly referred to as the charge relay system(Dodson and Wlodawer 1998; Delmarcelle et al. 2005a; Polgár 2005). In contrast, variations in the architecture of the active site, such as the Ser/Ser/Lys triad and Ser/Lys dyad, have also been reported (Paetzel and Dalbey 1997; Hedstrom 2002b; Shin et al. 2003; Paetzel

and J. Strynadka 2008). Recently, we found a new serine peptidase, D-stereospecific amidohydrolase (DAH) from *Streptomyces* sp. 82F2 (Arima et al. 2011a). The enzyme belongs to the S12 peptidase family, which has a catalytic Ser/Lys dyad (Ser86 and Lys89). The most characteristic feature of DAH is the recognition of D-amino acyl derivatives as substrates and the formation of amide bonds by aminolysis. In DAH aminolysis reactions, the enzyme preferentially uses D-aminoacyl derivatives as acyl donors and L-amino acids and their derivatives as acyl acceptors and produces dipeptides with a DL-configuration(Arima et al. 2011b). In fact, DAH has been used to synthesize a cyclic dipeptide as the lead compound of the pesticide cyclo-(D-Pro-L-Arg), which inhibits family 18 chitinases (Houston et al. 2002), in a one-step/one-pot reaction (Arima et al. 2011b).

Several of the enzymes of the S12 family exhibit high aminolysis activity toward various types of substrates including amides, esters, and peptides (Kato et al. 1989, 1990; Pratt and Frère 2013). The functions are thought to be mainly associated with the biosynthesis or remodeling of peptidoglycan. Five crystal structures of S12 family peptidases, including DAH (PDB: 3WWX), have been reported to date: D-aminopeptidase (PDB: 1EI5), D, D-peptidase (PDB: 3PTE), class C β-lactamase (PDB: 1BLS), D-amino acid amidase (PDB: 2EFX) (Lobkovskya et al. 1994; Kelly and Kuzin 1995; Bompard-Gilles et al. 2000; Okazaki et al. 2007; Arima et al. 2016). Among them, D, D-peptidase and D-stereospecific aminopeptidase, as well as DAH, catalyze the formation of peptide bonds by aminolysis(Kato et al. 1990; Bompard-Gilles et al. 2000). Their substrate specificities vary, and the structural factors responsible for the substrate specificity of hydrolysis have been identified (Delmarcelle et al. 2005b; Sauvage et al. 2008) However, the mechanisms of substrate (both acyl donors and acceptors) recognition for aminolysis remain

unclear but represent an important issue for understanding the characteristics of this class of enzymes and their detailed function in biosynthesis or remodeling of peptidoglycan.

Crystallographic analysis of DAH revealed that the enzyme possesses a large cavity. The side chains of Ser86 and Lys89 that create the catalytic Ser/Lys dyad are positioned at the center bottom of the cavity (Arima et al. 2016). In addition, there is a pocket close to this catalytic center (Fig.3.1). The overall structures of S12 enzyme family members are similar, although there are significant differences in terms of the shapes and sizes of the cavities and active site pockets among them. DAH recognizes L-aminoacyl derivatives specifically as acyl acceptors. However, the exact positions that recognize L-amino acids in the cavity of DAH have not been found. Okazaki et al. reported that the structure of the D-amino acid amidase pocket fits L-Phe and D-Phe (Okazaki et al. 2008a). In this structure, unlike the bound D-Phe, the bound L-Phe does not form an acyl-enzyme intermediate. Thus, we assumed that the pocket functions to recognize acyl acceptors for aminolysis. In addition to L-aminoacyl derivatives, DAH recognizes 1,8-diaminooctane (1,8-DAO) as an acyl acceptor in aminolysis (Arima et al. 2016), and the crystal structure of DAH has been refined in the presence of 1,8-DAO. Although the bound 1,8-DAO in the DAH crystal structure is positioned at the side of the cavity (Fig. 2.1), the distance between Ser86 and 1,8-DAO is 7.3 Å, which is too great for nucleophilic attack. Therefore, the 1,8-DAO binding form is thought not to reflect the location of the nucleophilic attack on the acyl acceptor (Arima et al. 2016). For that reason, an investigation into the effects of mutations of residues constituting the pocket on aminolysis could provide new insights. The aim of this study was to evaluate the role of the residues constituting the DAH pocket via mutations. We used site-directed mutagenesis to analyze the potential effects of altered residues in the DAH pocket, which is thought to bind substrates and investigated any changes in substrate recognition,

especially in aminolysis. The data indicated that Ile338 is an important residue for substrate recognition among the DAH pocket residues.

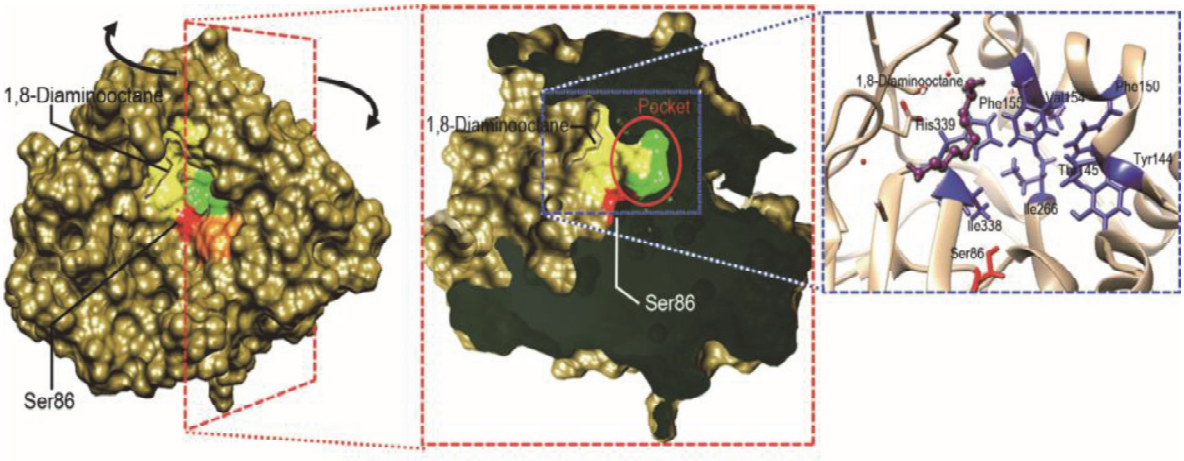

Fig. 2.1 Cavity shape and residues in the active site pocket. The pictures show the overall structure (left), a cross-sectional view (center), and a close-up view of D-stereospecific amidohydrolase (DAH). The bound 1,8-diaminooctane (1,8-DAO) molecule is shown as a stick or ball and stick. The active site Ser86 residue is shown in red, the residues composing the active site are shown in green (left and center) or blue, and the region associated with 1,8-DAO binding is shown in yellow.

2.2 MATERIALS AND METHODS

2.2.1 Materials, bacterial strains, and plasmids

Peptides and aminoacyl ester derivatives were purchased from Bachem AG, Aldrich Chemical Co. Inc., Sigma Chemical Co., Novabiochem Corp., and Wako Pure Chemical Industries Ltd. *Escherichia coli* JM109 was used as a host strain for general cloning procedures and *E. coli* Rosetta (DE3) was used as a host strain for gene expression. Plasmid pET-82F2DAP (with the *DAH* gene inserted into the MscI-NcoI gap of pET-22b (Arima et al. 2011b) was used for the expression of wild-type DAH (WT) and as a template for mutagenesis.

2.2.2 Enzyme assay

For routine assays, enzyme activity was determined via a continuous spectrophotometric assay with D-Phe-pNA as the substrate. Substrate solution (10 μL; 10 mM) was added to 90 μL of a mixture containing 200 mM Tris-maleate (pH 6.5) and 5 $\mu g \cdot mL^{-1}$ of the enzyme at 25 °C. The increased absorption at 405 nm caused by the release of pNA was monitored continuously with a microtiter plate reader (680; Bio-Rad Laboratories Inc.). The initial activity rate was determined from the linear part of the optical density profile of pNA measured using the same instrument.

2.2.3 Mutagenesis

Site-directed mutagenesis for the construction of mutant enzymes was conducted by inverse PCR using two pairs of primers containing a point mutation (Table 2.1). The PCR program consisted of 18 cycles for 1 min at 95 °C, 1 min at 65 °C, and 8 min at 68 °C. The PCR product was treated with Dpn I at 37 °C overnight. Thereafter, it was transfected into competent *E. coli* JM109 cells according to the manufacturer's protocol. After the plasmid was extracted, accurate cloning was confirmed by sequencing.

2.2.4 Expression and purification of WT and mutant enzymes

E. coli Rosetta (DE3) harboring pET-82F2DAH or the expression vector for mutant DAH production was cultivated at 25 °C for 48 h in 50 mL of Overnight Expression Instant TB medium (Novagen Inc.). Since DAH is an extracellular enzyme (Arima et al. 2011a), the culture was centrifuged to remove the cells and the recombinant enzyme was purified using the

following procedures. The culture supernatant was dialyzed against 20 mM sodium citrate (pH 5.5). The dialysate was loaded onto a Vivapure-S spin column (Sartorius AG) equilibrated with 20 mM sodium citrate (pH 5.5). After washing with the same buffer containing 0.1 M NaCl, the bound protein was eluted with the same buffer, this time containing 0.4 M NaCl. The homogeneity of the purified proteins was confirmed by 12% SDS-PAGE under denaturing conditions (Laemmli 1970).

2.2.5 Assay of aminolysis activity

Aminolysis and hydrolysis reactions are competitive and hydrolysis tends to occur at high temperatures; thus, the reaction was conducted at 4 °C to suppress hydrolysis. In addition, pH 8.5 was adopted for the aminolysis reaction to avoid the non-enzymatic degradation of ester substrates. The aminolysis activity of DAH was assayed as follows. First, 5 μL (or 50 μL) of 0.1 $mg \cdot mL^{-1}$ enzyme solution was added to 40 μL (or 400 μL) of the mixture containing 35 μL (or 350 μL) of 0.5 M Tris-HCl (pH 8.5) and 5 μL (or 50 μL) of 0.5 M 1,8-DAO. The reaction was initiated by adding 5 μL (or 50 μL) of an acyl donor substrate (aminoacyl derivative solutions dissolved in dimethyl sulfoxide at an appropriate concentration [ca. 0.5 M]). The reaction was then continued at 4 °C for 2–30 min. The reaction was terminated by adding 50 μL (or 500 μL) 0.5 M HCl to the mixture. The reaction mixture was then analyzed by measuring the released methanol and the weight of the reaction product, and by using mass spectrometry (MS).

Table 2.1 Sequences of primers used for site-directed mutagenesis

Mutations	Primer name	Sequence (5' to 3')
Y144A	DAH Y144A_F	CATCTACAGCGCGACCGAGGACCCCGCCTT
	DAH Y144A_R	AAGGCGGGGTCCTCGGTCGCGCTGTAGATG
T145A	DAH T145A_F	ATCTACAGCTACGCCGAGGACCCC
	DAH T145A_R	GGGGTCCTCGGCGTAGCTGTAGAT
F150A	DAH F150A_F	AGGACCCCGCCGCGCAGGCCAAGGTCTT
	DAH F150A_R	AAGACCTTGGCCTGCGCGGCGGGGTCCT
V154A	DAH V154A_F	TTCCAGGCCAAGGCGTTCGGCCCCGGCTT
	DAHV154A_R	AAGCCGGGGCCGAACGCCTTGGCCTGGAA
F155A	DAH F155A_F	GCCAAGGTCGCCGGCCCCGGCTTC
	DAHF155A_R	GAAGCCGGGGCCGGCGACCTTGGC
I266A	DAH I266A_F	CTCAACCCGAGCGCCGCGGGCGCG
	DAH I266A_R	CGCGCCCGCGGCGCTCGGGTTGAG
I338A	DAH I338A_F	CACGGCGGCGGCGCCCACGGCTCG
	DAHI338A_R	CGAGCCGTGGGCGCCGCCGCCGTG
H339A	DAH H339A_F	GGCGGCGGCATCGCCGGCTCGTCC
	DAH H339A_R	GGACGAGCCGGCGATGCCGCCGCC
I338G	DAH I338G_F	ACGGCGGCGGCGGCCACGGCTCGT
	DAH I338G_R	ACGAGCCGTGGCCGCCGCCGCCGT
I338S	DAH I338S_F	ACGGCGGCGGCAGCCACGGCTCGT
	DAH I338S_R	ACGAGCCGTGGCTGCCGCCGCCGT
I338D	DAH I338D_F	ACGGCGGCGGCGACCACGGCTCGT
	DAH I338D_R	ACGAGCCGTGGTCGCCGCCGCCGT
I338F	DAH I338F_F	ACGGCGGCGGCTTCCACGGCTCGT
	DAH I338F_R	ACGAGCCGTGGAAGCCGCCGCCGT

2.2.6 Measurement of the weight of the aminolysis product

DAH reaction mixtures for aminolysis sometimes appear as white precipitates. Before the reaction, the weights of the reaction tubes were measured and used as the basis weight of the reaction container. After the reaction, the precipitates were collected by centrifugation (13000 × *g*, 10 min) and dried at 60 °C for around 1 day. The weights of the dried products were measured by using an analytical balance (ATX84; Shimadzu).

2.2.7 MS analysis

The molecular masses of the products of DAH catalytic activity were determined via matrix-assisted laser desorption ionization–time-of-flight (MALDI-TOF) MS and electrospray ionization (ESI–TOF) MS. For MALDI-TOF MS analysis, the precipitates were collected by centrifugation (13000 × *g*, 10 min) and washed twice with distilled water. They were then suspended in 5 μL of MALDI matrix solution (150 mM 2, 5-dihydroxybenzoic acid in 50% acetonitrile). A small amount of each sample (ca. 1 μL) was dropped onto the target frame and dried, and the samples were analyzed using Autoflex TOF (Bruker Daltonics Inc.).

For ESI-TOF MS analysis, the reaction mixture was diluted with a 200-fold volume of 0.1% formic acid. After the solution was filtered, 5 μL from each sample was analyzed by using an ESI-TOF MS system (LCT Premier XE or Quattro Micro API; Waters Corp.). The data were processed using a computer program (MassLynx; Waters Corp.).

2.2.8 Methanol release assay

Liberated methanol, which is equivalent to the formation of the acyl-enzyme intermediate in the first step of the catalytic reaction, was measured with the 4-aminoantipyrine phenol method (Allain et al. 1974) coupled with an alcohol oxidase reaction. The DAH reaction mixture (10 µL) was added to 90 µL of the mixture containing 140 mM Tris-HCl (pH 8.0), 0.5 mM 4-aminoantipyrine, 2 mM phenol, 0.1 $mg \cdot mL^{-1}$ horseradish peroxidase, and 0.1 $mg \cdot mL^{-1}$ alcohol oxidase. Absorbance was determined at 490 nm using a microtiter plate reader (680; Bio-Rad Laboratories Inc.) after incubation for 30 min at room temperature. The concentration of the liberated methanol was measured from the linear part of the optical density profile of standard methanol using the same instrument.

2.2.9 Thermal stability test

The thermal stability of wild-type and mutant DAHs was investigated as follows: the purified enzyme solution (0.1 mg/mL) was incubated for 30 min at temperatures of 30–60^{o}C. Subsequently, the samples were assayed for residual activity using the methanol release activity assay described above.

2.2.10 Structural model of mutant DAHs

The sequences of the primary structures of the mutant DAHs were aligned with the sequences of the WT (Protein Data Bank accession no. 3WWX). The alignment data were submitted to SWISS-MODEL (Arnold et al. 2006a; Biasini et al. 2014a) to generate a homology model of mutant DAHs based on the template structure of WT. The structural models obtained were analyzed using UCSF Chimera software (Arnold et al. 2006a).

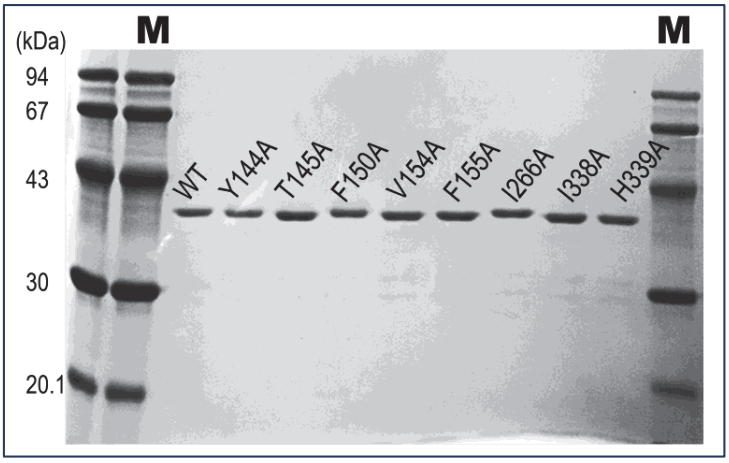

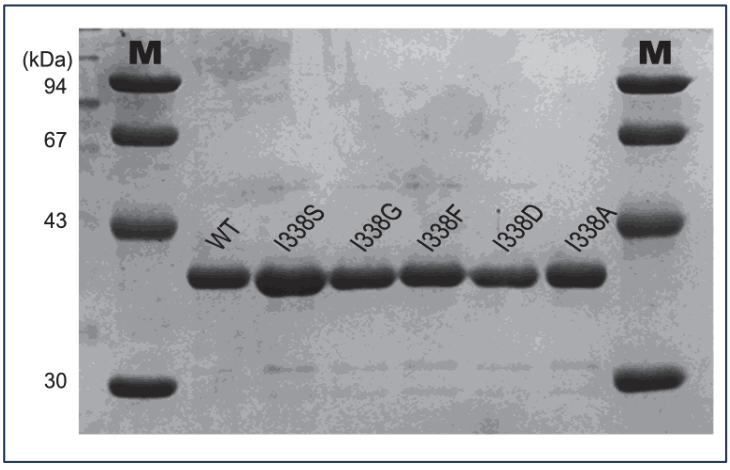

Fig. 2.2 SDS-PAGE of partially purified wild-type (WT) and mutant D-stereospecific amidohydrolases (DAHs). Samples (3 μg) were loaded on a 12% gel.

2.3 RESULTS

2.3.1 Effect of the mutation of residues of the pocket on pNA-releasing activity

DAH possesses a small pocket close to the catalytic center of Ser86 (Arima et al. 2016) (Fig. 2.1). The space, shape, and electrostatic environment of the pocket are believed to confer the substrate specificity of DAH. To elucidate the way that the pocket relates to the substrate specificity, especially during the aminolysis reaction of DAH, we performed mutational analysis focusing on the residues in the pocket. Based on the crystal structure of DAH, eight residues (Tyr144, Thr145, Phe150, Val154, Phe155, Ile266, Ile338, and His339) that constitute the pocket (Fig. 2.1) were selected and substituted with alanine. As judged by SDS-PAGE, all mutants could be purified as described in the Materials and Methods section (Fig. 2.2). The release of pNA is accompanied by the formation of an acyl-enzyme intermediate (Fig. 2.3A). We first assessed the effect of the mutation on pNA-releasing activity with D-Phe-pNA. Mutants release of pNA by D-Phe-pNA at pH 8.5 tended to be higher or at the same level as that at pH 6.5, whereas that by the WT showed optimum activity at pH 6.5 (Fig. 2.3B). The results indicated that the optimum pH for the formation of the acyl-enzyme intermediate was shifted to alkaline especially in the mutants of (Y144, T145, F150, I266, and I338).

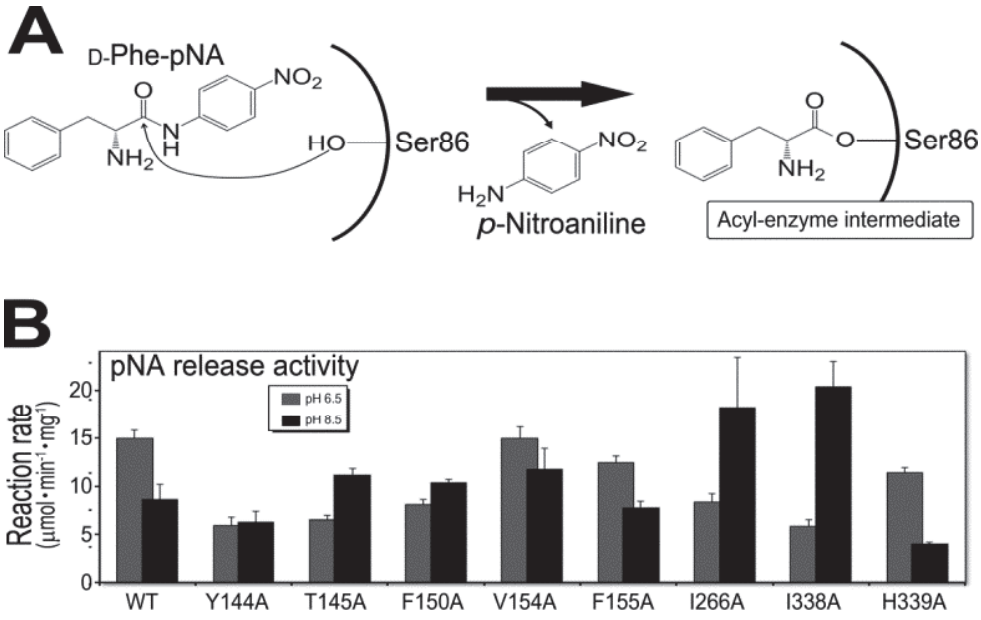

Fig. 2.3 Effect of mutation on p-nitroanilide (pNA) release activity from D-Phe-pNA. (A) Reaction scheme of the pNA release via DAH. (B) pNA release activity of the wild-type (WT) and mutant DAHs. *p*-Nitroaniline is a product of the formation of the acyl-enzyme intermediate when D-Phe-pNA is used as a substrate. The reaction was performed in a solution containing 1 mM D-Phe-pNA at pH 6.5 (gray bars) or 8.5 (black bars) at 25 °C. Each value represents the mean ± standard deviation (SD) of values from four independent experiments.

2.3.2 Effects of the mutation of residues in the pocket on aminolysis activity

DAH possesses a small pocket close to the catalytic center of Ser86 (Arima et al. 2016) (Fig.2.1). The space, shape, and electrostatic environment of the pocket are believed to confer the substrate specificity of DAH. To elucidate the way that the enzyme pocket relates to substrate specificity, especially during aminolysis reactions of DAH, we performed mutational analysis focusing on the residues in the pocket. Based on the crystal structure of DAH, eight residues (Tyr144, Thr145,

Phe150, Val154, Phe155, Ile266, Ile338, and His339) that constitute the pocket (Fig. 2.1) were selected and substituted with alanine. SDS-PAGE confirmed the purity of all mutants as described in the Materials and Methods section (Fig. 2.2). To investigate the possible effects of mutations on aminolysis, we examined the products of the enzyme reaction by using Ac-D-Phe methyl ester (Ac-D-Phe-OMe) in combination with 1,8-DAO as the acyl-donor and acyl-acceptor substrates, respectively, under optimum conditions for aminolysis (i.e., at 4 °C and pH 8.5) (Arima et al. 2011a).

In the reaction mixtures of each enzyme, precipitates appeared after several minutes (Fig.2.5). MS analysis showed that these precipitates were composed of the condensation products of Ac-D-Phe-OMe and 1,8-DAO, Ac-D-Phe-1,8-DAO, and Ac-D-Phe-1,8-DAO-Ac-D-Phe (Fig.2.5). Therefore, we assumed that precipitation represented the catalytic activity for aminolysis (Fig. 2.4A). As portrayed in Fig. 2.4B–2.4D, the same level of methanol release (acyl-enzyme intermediate formation) but a lower level of Ac-D-Phe formation (hydrolysis) and a higher level of precipitation formation (aminolysis) were observed in a 15-min reaction with the I338A mutant. The results indicated that DAH aminolysis was enhanced by substitution of Ile338 with Ala.

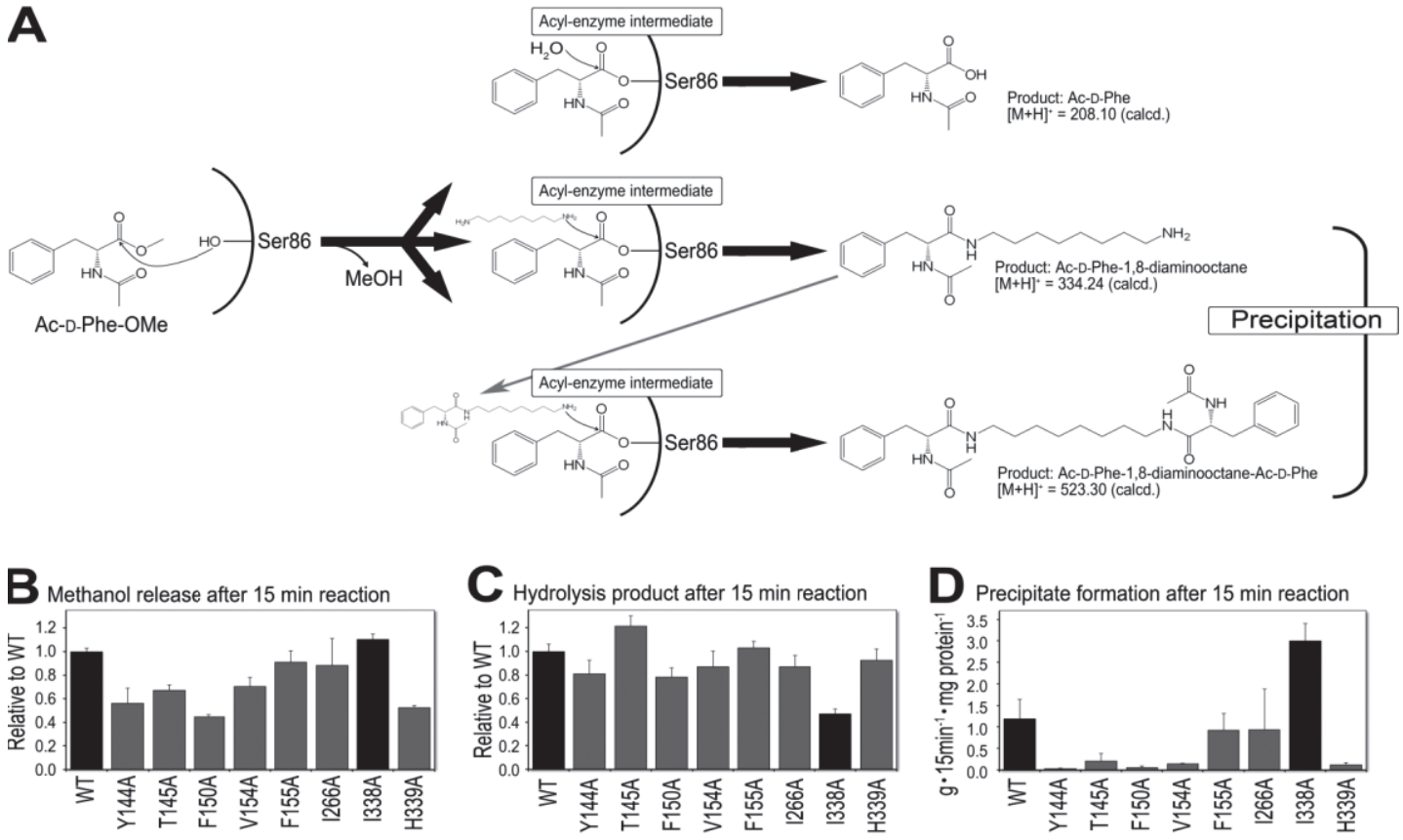

Fig. 2.4 Effects of mutation on methanol release, hydrolysis, and aminolysis. (A) Scheme of the DAH reaction using Ac-D-Phe methyl ester (Ac-D-Phe -OMe) and 1,8-DAO as the acyl donor and acceptor substrates, respectively. (B) Methanol release of the WT and mutant DAHs. Methanol is a product of the formation of the acyl-enzyme intermediate when Ac-D-Phe-OMe is used as a substrate. The values were calculated from the concentration of methanol after 15-min enzyme reactions. (C) Comparison of the concentrations

of hydrolysis reaction products after 15 min with the WT and mutant DAHs. (D) Precipitation formation activity of the WT and mutant DAHs. Precipitates were assumed to be a product of aminolysis. The values were calculated from the weights of the precipitates after 15-min enzyme reactions. In all graphs, the reactions were performed in solutions containing 20 mM Ac-D-Phe-OMe and 50 mM 1,8-DAO at pH 8.5 and 4 °C for 15 min. Each value represents the mean ± SD of values from four independent experiments.

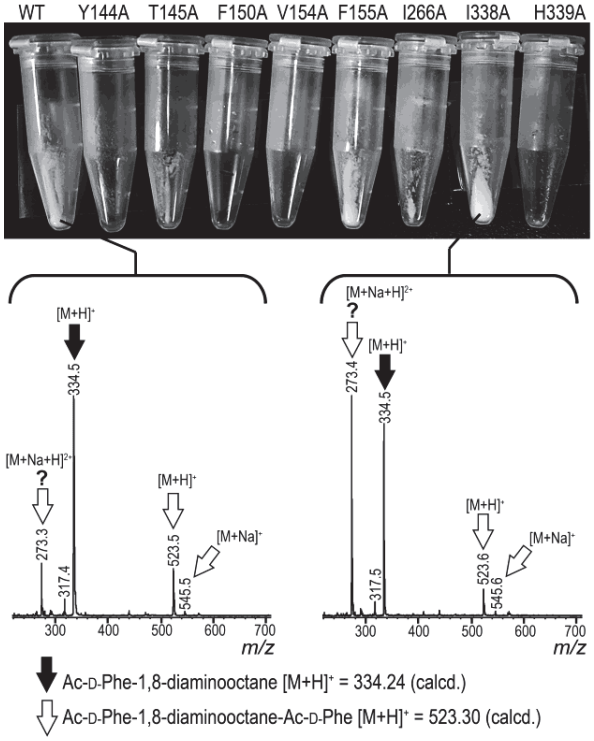

Fig. 2.5 Precipitates in the reaction mixtures of WT and mutant DAHs representing aminolysis reactions. The precipitates appeared in the reaction mixture (500 μL) several minutes after the reaction started. The reaction was performed in a solution containing 20 mM Ac-D-Phe methyl ester (Ac-D-Phe -OMe) and 50 mM 1,8-diaminooctane (1,8-DAO) at pH 8.5 and 4 °C for 15 min. Photographs were taken after centrifugation to obtain the precipitates.

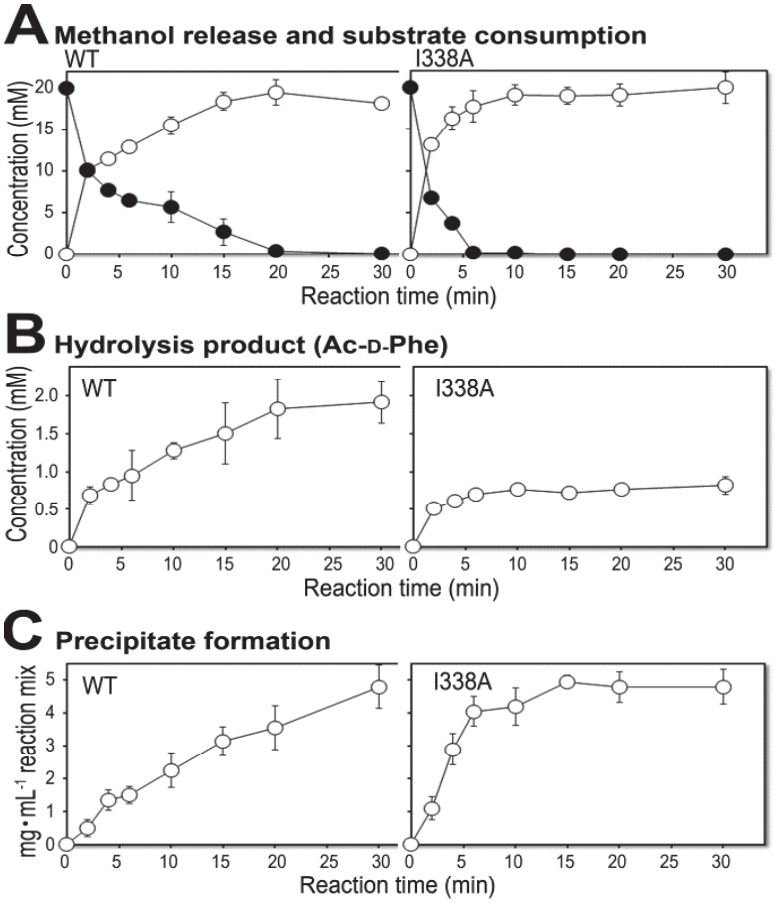

Fig. 2.6 Time dependence of the reaction products by catalysis with the WT and I338A DAHs. (A) Methanol release and substrate consumption. Open circles show the concentrations of methanol; closed circles show the concentrations of Ac-D-Phe-OMe. (B) Concentrations of hydrolysis products after the respective reaction times. (C) Weights of the precipitates after the respective reaction times. All graphs represent reactions performed in solutions containing 20 mM Ac-D-Phe-OMe and 50 mM 1,8-DAO at pH 8.5 and 4 °C. Each value represents the mean ± SD of values from four independent experiments.

2.3.3 Properties of I338A DAH from an aminolysis point of view

We focused on I338A DAH, which showed the strongest mutational effect on aminolysis, and investigated the properties of this mutant in detail. Figure 2.6 shows the time courses of Ac-D-Phe-OMe consumption, methanol release (acyl-enzyme intermediate formation), hydrolysis product release, and aminolysis product release when Ac-D-Phe-OMe and 1,8-DAO were used as substrates. The release of methanol and consumption of the substrate with I338A were higher than those with the WT (Fig. 2. 6A). In contrast, the production of Ac-D-Phe (hydrolysis product) was lower with I338A than with WT, as portrayed in Fig. 2.6B. The lower productivity of Ac-D-Phe in the I338A reaction was presumed to be caused by a lower susceptibility to nucleophilic attack by water or an increase in susceptibility to nucleophilic attack by 1,8-DAO on the acyl-enzyme intermediate via the mutation. In addition, the rate of precipitation with I338A was higher than that with the WT and quickly reached saturation (10 min, Fig. 2.6C). The results indicated that modification of the 338 Ile side-chain structure led to enhanced aminolysis activity.

The effects of 1,8-DAO concentration on methanol release, hydrolysis, and aminolysis activity for WT and I338A were assessed. The results showed lower hydrolysis activity for I338A compared with WT (Fig.2.7). In contrast, methanol release, which was thought to reflect an increase in the reaction rate for Ac-D-Phe-1,8-DAO production, was much higher for I338A than WT.

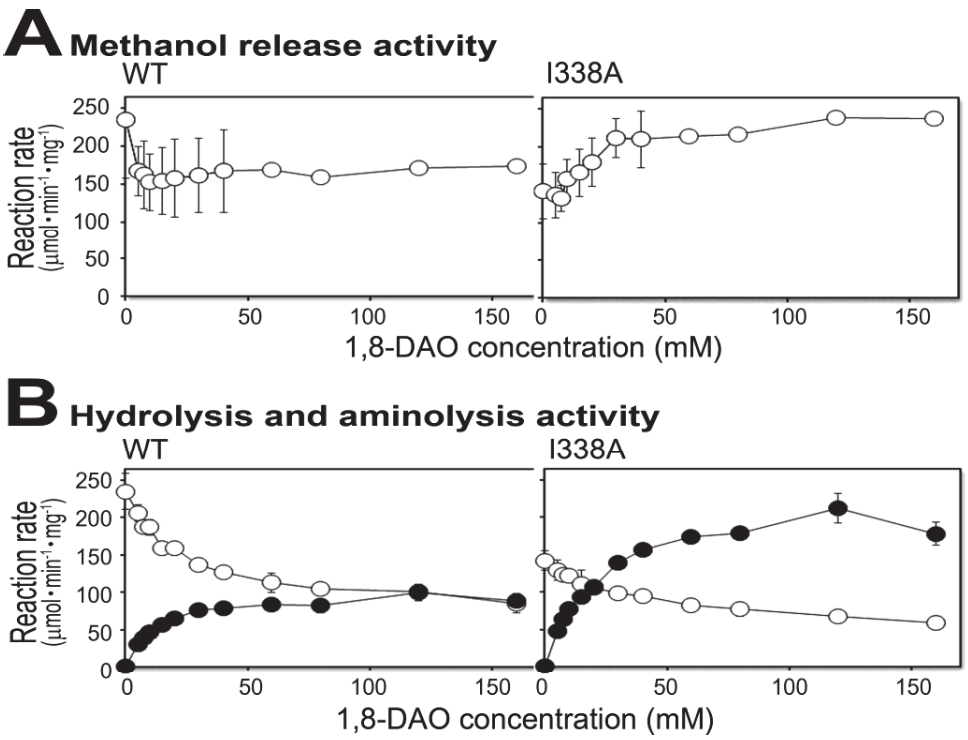

Fig. 2.7 Effect of 1,8-DAO on methanol release (A), hydrolysis (B), and aminolysis (B) of WT and I338A DAHs. (B) Open circles, the reaction rate for Ac-D-Phe production; closed circles, reaction rates for Ac-D-Phe-1,8-DAO production. Reactions were performed in a solution containing 20 mM Ac-D-Phe-OMe at pH 8.5 and 4°C for 5 min. Each value represents the mean ± standard deviation of values from eight independent experiments.

2.3.4 Enzyme kinetics

We further examined the enzyme kinetics of the aminolysis and hydrolysis reactions of I338A and the WT. As summarized in Table 2.2, The k_{cat} for methanol release was related to only Ac-D-Phe-OMe; that is, the theoretical max value for the nucleophilic attack of DAH on Ac-D-Phe-OMe. In contrast, the k_{cat} values for hydrolysis and aminolysis are the theoretical max values for the nucleophilic attack of water and 1,8-DAO, respectively. Therefore, the rate-limiting step in this enzyme reaction is the formation of the acyl-enzyme intermediate Table 2.2: the k_{cat} of I338A for methanol release from Ac-D-Phe-OMe increased on addition of 1,8-DAO (from 80.1 s^{-1} to 304 s^{-1}) and the K_m value of I338A for methanol release from Ac-D-Phe-OMe also changed (from 3.78 mM to 19.5 mM). In contrast, the k_{cat} and K_m of the WT for methanol release from Ac-D-Phe-OMe under the respective conditions remained almost the same (k_{cat}: 96.4–95.2 s^{-1}, K_m: 3.30–4.95 mM).

In terms of Ac-D-Phe-OMe hydrolysis, the changes in k_{cat} of both enzymes on the addition of 50 mM 1,8-DAO were almost identical (WT changed from 96.4 s^{-1} to 46.7 s^{-1}, and I338A from 80.1 s^{-1} to 43.7 s^{-1}). However, the apparent K_m of I338A increased on addition of 1,8-DAO (from 3.78 mM to 7.07 mM), while that of WT decreased (from 3.30 mM to 2.01 mM). Thus, the kinetics of DAH aminolysis were dramatically affected by the mutation. The k_{cat} value of I338A under the respective fixed conditions (50 mM 1,8-DAO or 50 mM Ac-D-Phe-OMe) was higher than that of the WT.

Table 2.2 Enzyme kinetics for hydrolysis and aminolysis by the WT and I338A DAHs. The reaction was performed at pH 8.5 for 2 min.

Reaction	Concentration of one substrate	k_{cat}[a] (s^{-1})		K_m for respective substrates[a] (mM)		
		WT	I338A	Substrate	WT	I338A
Methanol releasing from Ac-D-Phe-OMe	0 mM 1,8-DAO	96.4 ± 10.5	80.1 ± 6.41	Ac-D-Phe-OMe	3.30 ± 0.23	3.78 ± 0.85
	50 mM 1,8-DAO	95.2 ± 3.2	304 ± 41	Ac-D-Phe-OMe	4.95 ± 0.58	19.5 ± 5.9
Ac-D-Phe-OMe hydrolysis (Ac-D-Phe production)	0 mM 1,8-DAO	-[d]	-[d]	Ac-D-Phe-OMe	-[d]	-[d]
	50 mM 1,8-DAO	46.7 ± 1.6	43.7 ± 3.1	Ac-D-Phe-OMe	2.11 ± 0.32[d]	7.07 ± 0.99[d]
aminolysis[b]	50 mM 1,8-DAO	43.6 ± 3.5	345 ± 26	Ac-D-Phe-OMe	7.58 ± 0.95[e]	34.8 ± 3.2[e]
	50 mM[c] Ac-D-Phe-OMe	91.0 ± 8.3	168 ± 27	1,8-DAO	7.47 ± 1.14	9.81 ± 2.36

[a] Values are calculated from a nonlinear regression fit to the Michaelis–Menten equation using initial estimates from double-reciprocal plots (1/S vs. 1/V). The values are expressed as the mean ± SD of four independent experiments.

[b] aminolysis: Production of Ac-D-Phe-1,8-DAO and Ac-D-Phe-1,8-DAO-Ac-D-Phe. The subtracted values of the reaction rates for Ac-D-Phe production from the reaction rates of methanol release were assumed to be the reaction rates for the production of Ac-D-Phe-1,8-DAO and Ac-D-Phe-1,8-DAO-Ac-D-Phe.
[c] The concentration was determined by the solubility of Ac-D-Phe-OMe in water.
[d] It was assumed that the values are almost the same as those of methanol released in 0 mM 1,8-DAO

[e] Apparent values calculated from nonlinear regression fitting to the Michaelis–Menten equation using initial estimates from double-reciprocal plots (1/S vs. 1/V).

2.3.5 Effects of the Ile338 mutation on enzyme activity and thermal stability

The effects of the structural modification of Ile338 on hydrolysis and aminolysis were examined by constructing several mutants (I338G, I338S, I338D, and I338F) and investigating the ability of each to form the acyl-enzyme intermediate and mediate aminolysis and hydrolysis. The purity of the mutants was assessed via SDS-PAGE (Fig. 2.2).

A different effect was observed in the investigation into methanol release, hydrolysis, and aminolysis of Ac-D-Phe-OMe in the presence of 1,8-DAO. Aminolysis via DAH was significantly enhanced by substitutions with Ala and Ser. That is, the mutants exhibited higher levels of methanol release (acyl-enzyme intermediate formation), lower hydrolysis activity, and a five-fold greater formation of precipitates than the WT (Fig. 2.8). Substitutions with Gly and Phe also moderately enhanced aminolysis. However, the acyl-enzyme intermediate formation of 1338F was lower than that of the WT. In contrast, substitution with Asp decreased the ability of DAH to form the acyl-enzyme intermediate and mediate–hydrolysis and aminolysis. This indicates that the introduction of a negative charge at position 338 of DAH negatively affects DAH activity in the presence of Ac-D-Phe-OMe.

We next examined the thermal stability of wild-type and mutant DAHs. As shown in Fig. 2.9, they exhibited slightly lower stability with respect to temperature (up to 45 ^{o}C) than the WT. Based on the results, the mutation of Ile338 might lead to a change in the local flexibility of the active site pocket.

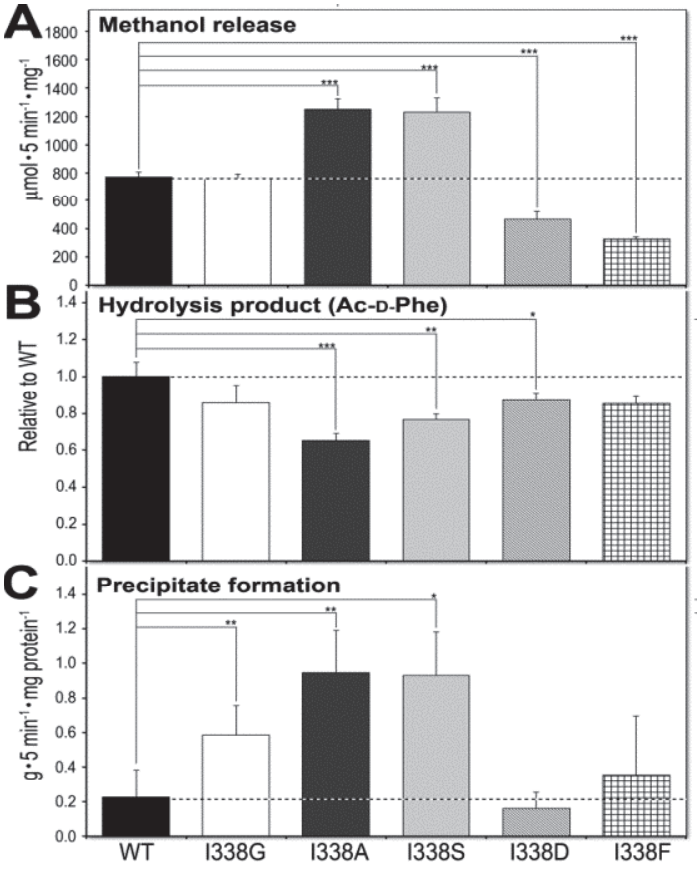

Fig. 2.8 Effects of Ile338 mutations on methanol release, hydrolysis, and aminolysis by DAH. (A) Methanol release via WT and mutant DAHs to Ac-D-Phe-OMe. The values were calculated from the concentrations of methanol. (B) Comparison of the concentrations of the hydrolysis products (Ac-D-Phe) of the WT and mutant DAHs. (C) WT and mutant DAHs precipitate formation activity. The values were calculated from the weights of the precipitates. All graphs represent comparisons of the products following reactions performed in solutions containing 20 mM Ac-D-Phe-OMe and 50 mM 1,8-DAO at pH 8.5 and 4 °C for 5 min (the length of the time that precipitation takes to occur without completion of the reactions). Each value represents the mean ± SD of values from four independent experiments.* $p < 0.05$; ** $p < 0.02$; *** $p < 0.01$ calculated by Student's *t* test.

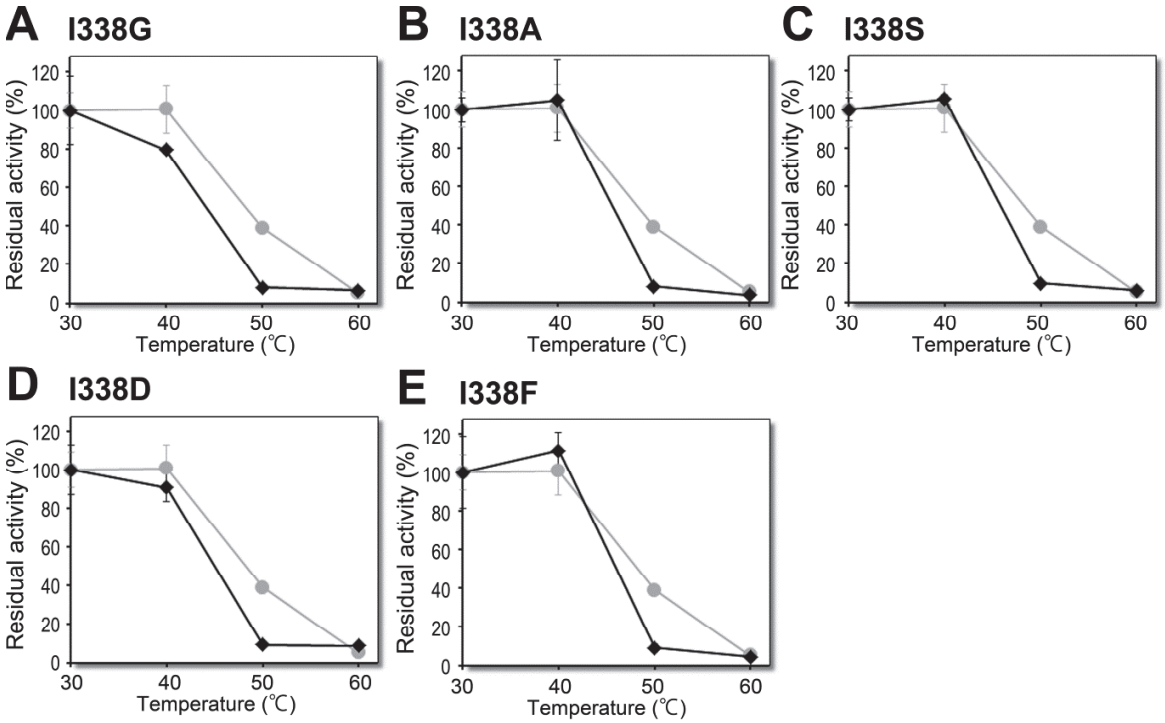

Fig. 2.9 Thermal stabilities of WT and mutant DAHs. Symbols in each panel: *gray circle* WT; *filled diamond* mutant enzyme. Each value represents the mean ± SD of values from four independent experiments.

2.3.6 Acyl acceptor preferences of WT and mutant DAHs

Finally, we examined the aminolysis ability of the WT and mutant DAHs using Ac-D-Phe-OMe as an acyl donor and several amino acids and peptides as acyl acceptors to investigate the changes in acyl acceptor specificities of the mutants. In this experiment, Gly, Gly-OMe, Gly-Gly ($(Gly)_2$), Gly-Gly-Gly ($(Gly)_3$), L-Leu, L-Leu ethyl ester (-OEt), L-Leu-L-Leu ($(Leu)_2$), L-Leu-L-Leu-L-Leu ($(Leu)_3$) were used as the acyl acceptor substrates.

Aminolysis was dramatically enhanced with mutations of Ile338 to Ala, Ser, and Phe when using L-Leu as an acyl acceptor (Fig. 2.10 B). In the reaction using Gly and glycyl peptides as acyl acceptors, several mutants (I338A, I338S, and I338F) exhibited enhanced aminolysis compared with the WT (approximately two-fold); the trends in the effects of the mutations were similar to the reaction using L-Leu and 1,8-DAO (Fig. 2.10 A). In contrast, the effects of mutations on aminolysis using Gly-OMe, leucyl peptides, and L-Leu-OEt differed from those using 1,8-DAO, amino acids (Gly and L-Leu), and glycyl peptides as acyl acceptors. The activity levels of all mutants were almost the same as that of the WT when using Gly-OMe as an acyl acceptor (Fig. 2.10 A). In the reaction using leucyl peptides as acyl acceptors, only I338F exhibited enhanced aminolysis compared with the WT (Fig. 2.10 A). In contrast, mutants other than I338F exhibited enhanced aminolysis with L-Leu-OEt as an acyl acceptor, which was in contrast to the reaction with leucyl peptides.

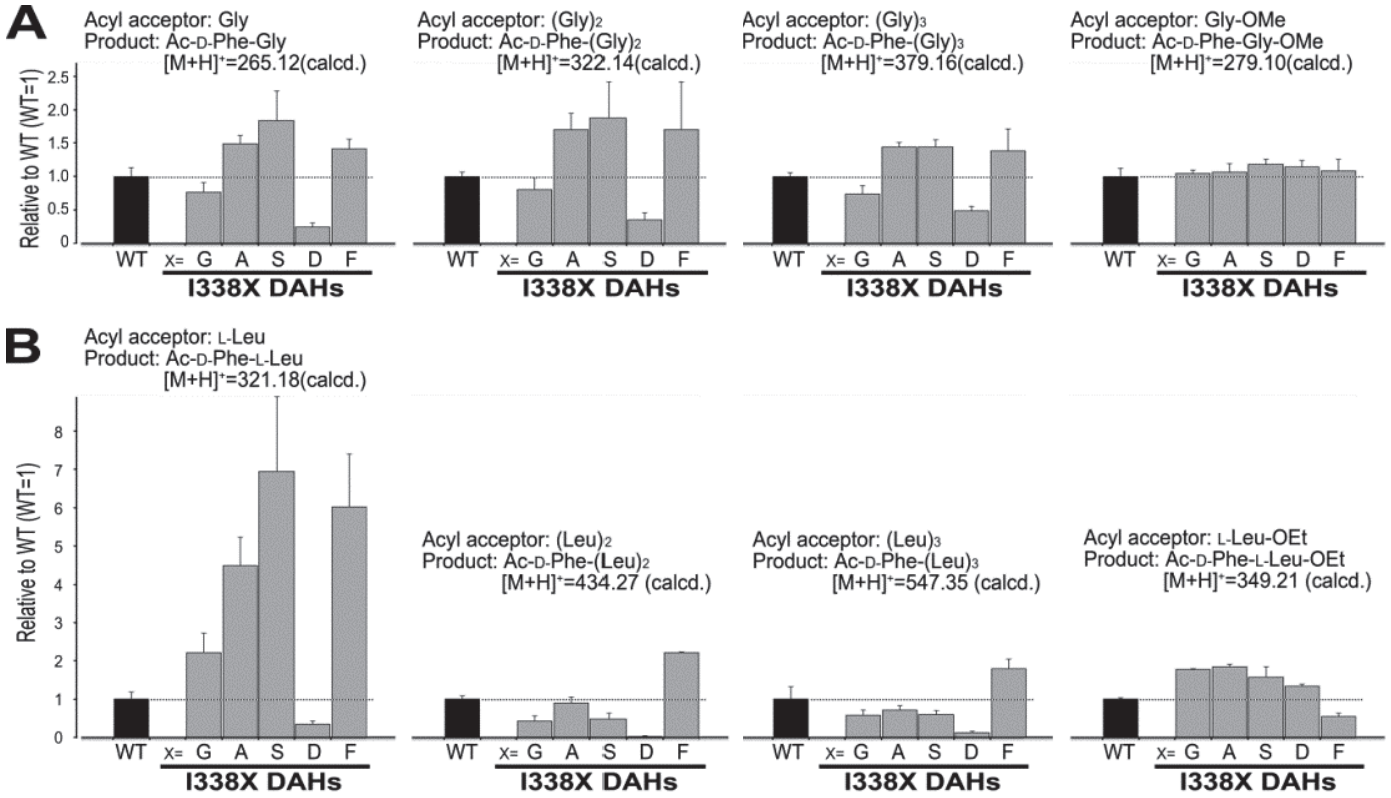

Fig. 2.10 Changes in the ratio of aminolysis products via the mutations. (A) Relative amounts of aminolysis products from reactions using Gly, glycyl peptides, or Gly-OMe. (B) Relative amounts of aminolysis products from reactions using L-Leu, leucyl peptides, or Leu ethyl ester (Leu-OEt). All graphs represent reactions performed in solutions containing 20 mM Ac-D-Phe-OMe and 50 mM acyl acceptor substrate at pH 8.5 and 4 °C for 5 min. Each value represents the mean ± SD of values from four independent experiments.

2.4 DISCUSSION

Among the overall structures of the S12 enzyme family members, significant differences are observed in the shapes and sizes of the cavities and pockets. In particular, the enzymes, including DAH, that catalyzes aminolysis, possess large cavities. Crystallographic analysis of DAH with 1,8-DAO indicates that 1,8-DAO binds to the middle of the cavity and the pocket and side chain of Ser86 in DAH are accessible to acyl donor substrates (Arima et al. 2016). Therefore, a large cavity is considered necessary to confer binding to the acyl acceptor without covering the active site Ser and its pocket.

DAH prefers L-amino acids and their derivatives as acyl acceptors and they cannot utilize D-amino acids (Arima et al. 2011b). This indicates that DAH recognizes only L-amino acids as acyl acceptors and bypasses D-amino acids. As described in the Introduction section, the pocket structure of DAA, which is homologous to that of DAH, fits L-Phe without the formation of an acyl-enzyme intermediate. Thus, we assumed that the pocket functions to recognize acyl acceptors for aminolysis. In this study, we found that recognition of the acyl acceptor in aminolysis is changed by substituting Ile338 with another residue.

Our results clearly demonstrated that substitution with Ala and Ser specifically led to a decrease in hydrolytic activity and an increase in aminolysis when 1,8-DAO was used as the acyl acceptor (Figs. 2.6 and 3.8). The k_{cat} and K_m values of WT for methanol release from Ac-D-Phe-OMe in the absence of 1,8-DAO were almost identical to those of I338A (Table 2.2). These results indicate that the DAH potentials for substrate affinity and the formation of an acyl-enzyme intermediate for Ac- -Phe-OMe are barely affected by the mutation. The K_m for methanol release increased after adding 1,8-DAO. This result is consistent with our previous reports (Arima et al. 2011b, 2016); that is, the increase in K_m implies that the binding of 1,8-DAO interferes with Ac-D-Phe-OMe binding to the enzyme. The K_m for methanol release of

I338A with Ac-D-Phe-OMe was dramatically increased via the addition of 1,8-DAO; however, that of the WT changed only slightly (Table 2.2). Thus the mutant is considered to have a high inclination to bind 1,8-DAO. The k_{cat} for methanol release of I338A was also dramatically increased by the addition of 50 mM 1,8-DAO; therefore, we presumed that the enhanced 1,8-DAO binding via mutation led to the increase in aminolysis activity.

In addition to the results using 1,8-DAO, a different effect on aminolysis activity by mutation was observed when leucyl peptides were used as acyl acceptor substrates. That is, the activities for leucyl peptides were apparently reduced by mutations of Ile338 to Gly, Ala, and Ser (Fig. 2.10). Among the eight residues that constitute the pocket, Ile338 exists at the position closest to the active center Ser (5.05 Å). Thus, mutations of Ile338 to Gly, Ala, or Ser presumably expand the space in the active center of the pocket. In addition, a thermal stability test indicated that the mutation might affect the local flexibility of the pocket near the active center Ser. According to the report of Fields (Fields 2001), molecular flexibility and rigidity are important characteristics in the activity and stability of proteins. In particular, the high structural flexibility of psychrophilic enzymes may allow better interactions with substrates and could explain their higher catalytic rate, lower thermostability, and lower activation energy requirements compared with those of mesophilic and thermophilic enzymes. Therefore, changes in local flexibility are considered to allow an increase in the ability to accommodate the acyl acceptor substrate (1,8-DAO), which leads to changes in aminolysis activity. Changes in the local environment have different effects among Ile338 mutants; thus, the effects on aminolysis mediated by Ile338 mutations also differ. In the I338F mutant especially, leucyl derivatives are accepted as preferable acyl acceptor substrates, whereas the steric space of the pocket seems to be narrower than that of the other mutants. Although we could not find a reason for the low

activity toward L-Leu-OEt, we speculated that a hydrophobic interaction between the side chain of position 338 and the alkali part of Leu derivatives might form in the I338F mutant.

The effects of the Ile338 mutations on the recognition of acyl acceptors were different (Figs. 2.8 and 2.10). Thus, the structure at position 338 is thought to specify the preferred acyl acceptors. In addition, I338F and I338D had a lower ability to form acyl-enzyme intermediates with Ac-D-Phe-OMe than the WT (Fig 2.8). The results indicated that the nucleophilicity of the catalytic center Ser86 or the affinity to Ac-D-Phe-OMe was weakened by mutations of Ile338 to Phe and Asp. Based on the results, the 338 position is presumably related to multiple functions of DAH's ability in aminolysis. It is conceivable that the shape, local flexibility, and electrostatic environment of the pocket are the ultimate determinants of the functions of DAH. Many hypotheses on the catalytic functions of DAH, including the formation of acyl-enzyme intermediates and recognition of acyl donor and acceptor substrates, remain unresolved and detailed studies are required for clarification.

2.5 CONCLUSION

In this study, we analyzed the effects of modifying the pocket structure of DAH on aminolysis and the accompanying processes, such as the recognition of substrates and the formation of acyl-intermediates. The results will contribute to our understanding of the structural basis of the substrate specificity and catalytic function of DAH. This study revealed the relationship between the pocket shape (i.e., expansion of the space, changes in local flexibility, and the electrostatic environment of the active center side on the pocket) and aminolysis. In addition, several findings related to enzyme function, such as the nucleophilicity of the catalytic center Ser86 or weakening of the affinity to Ac-D-Phe-OMe via mutations of Ile338 were unclear.

Therefore, a future challenge will be to modify other parts of the pocket or cavity through mutations to clarify the relationship between the function of DAH and the pocket/cavity structure.

CHAPTER THREE

EFFECT OF ACTIVE SITE POCKET STRUCTURE MODIFICATION OF D-STEREOSPECIFIC AMIDOHYDROLASE ON THE RECOGNITION OF STEREOSPECIFIC AND HYDROPHOBIC SUBSTRATES

3.1 INTRODUCTION

Serine peptidases function in a wide range of physiological processes, such as digestion, protein maturation and turnover, homeostasis, and immune responses (Page and Di Cera 2008). Almost one-third of all peptidases can be classified as serine peptidases, named for the nucleophilic Ser residue at the active site (Hedstrom 2002a). The catalytic mechanism of serine peptidases appears to be conserved among the members of this extensive family. First, a covalent acyl-enzyme intermediate is generated with a substrate that is an acyl donor. Next, the intermediate undergoes nucleophilic attack by water or amino groups (termed aminolysis). In the latter step of this reaction, water or an amino group acts as an acyl acceptor. The diverse activities of serine peptidases are the result of different sets of amino acids utilized for substrate binding (Craik et al. 1985), with several peptidases preferring peptides consisting of D-amino acids, aminoacyl amides, or esters (Asano and Lübbehüsen 2000; Goswami and Van Lanen 2015).

The D-stereospecific amidohydrolase from *Streptomyces* sp. 82F2 (DAH) is a serine peptidase (family S12 in MEROPS (Rawlings et al. 2016) and recognizes D-amino acyl derivatives mainly as acyl donor substrates. The enzyme exhibits high aminolysis activity as a side reaction in accordance with its hydrolysis activity. DAH mainly recognizes D-aminoacyl ester derivative substrates during both hydrolysis and aminolysis catalysis (Arima et al. 2011a) yet preferentially uses L-amino acids and their derivatives as acyl acceptors in aminolysis

reactions, making this enzyme of particular interest for synthesizing dipeptides with a DL-configuration. Indeed, DAH has been used to synthesize the cyclic dipeptide cyclo (D-Pro-L-Arg) in a one-step/one-pot reaction (Arima et al. 2011b) as the lead compound of a pesticide which inhibits family 18 chitinases (Houston et al. 2002). In contrast, DAH shows only moderate activity to L-form hydrophobic/aromatic amino acid derivatives during acyl-enzyme intermediate formation; that is, DAH recognizes L-form hydrophobic amino acid derivatives as an acyl donor substrate (Arima et al. 2011a). Therefore, the stereoselectivity of DAH for acyl-enzyme intermediate formation is not strict only to D-form substrate.

Crystallographic analysis of DAH (PDB: 3WWX) revealed a large cavity that leads to the active center (Arima et al. 2016). In addition, there is a pocket near the active center residues Ser86 (Fig. 3.1A and B). This pocket may play functional roles in substrate recognition but the relationship between this pocket and substrate recognition (stereoselectivity and preference for hydrophobic substrates) remains unclear. An investigation into the effects of mutation of the active site on the stereoselectivity and the preference of DAH for hydrophobic substrates could, therefore, provide new insights into catalysis by this enzyme. Understanding the mechanism underlying substrate recognition is important for the rational modification of enzymes aimed at developing a convenient biocatalyst for peptide synthesis with controlled configuration.

D-Amino acid amidase (DAA, PDB: 2EFX) belongs to the same family as DAH and has an active site pocket similar in size and shape to that of DAH (Okazaki et al. 2007). The DAA pocket can accommodate D-Phe and forms an acyl-enzyme intermediate. Glu114 in DAA supplies a negative surface charge for recognizing the N-terminus of the substrate. Ala239 and Gly243 are located at the bottom of the hydrophobic pocket and likely interact with the D-Phe phenyl ring, thereby providing important insights into understanding the mechanism of substrate

recognition by this family of enzymes. Specifically, the shape and electrostatic environment of the pocket are likely related to substrate preference(John J. Perona and Charles S. Craik 1995; Tsai et al. 2010) The residues Thr145, Ala267, and Gly 271 in DAH correspond to Glu114, Ala239, and Gly243 in DAA, respectively (Fig. 3.2 A), and therefore Thr145, Ala267, and Gly 271 in DAH are likely involved in recognizing the substrate.

In this study, we focused on Ala267, Gly271, and Thr145 in DAH for assessing the effect of size/shape changes to the pocket on its stereoselectivity. The residues were replaced with the bulky amino acid residue Phe, and then we evaluated the effect of each mutation on the ability of the enzyme to form acyl-enzyme intermediates with the model substrates L- and D-Phe-methyl ester (-OMe), and acetyl- (Ac-) L- and D-Phe-OMe. We found that mutation of position 267 located at the bottom of the site active pocket of DAH affects the enzyme's substrate stereoselectivity.

3.2 MATERIALS AND METHODS

3.2.1 Materials, bacterial strains, and plasmids

Amino acid derivatives were purchased from Bachem AG (Bubendorf, Switzerland), Aldrich Chemical Co., Inc. (Milwaukee, USA), Sigma Chemical Co. (St. Louis, MO, USA), Novabiochem Corp. (San Diego, California, USA), Wako Pure Chemical Industries Ltd. (Osaka, Japan), and Tokyo Chemical Corp. (Tokyo, Japan). *Escherichia coli* JM109 was used as a host strain for general cloning procedures and *E. coli* Rosetta (DE3) was used as a host strain for gene expression. Plasmid pET-82F2DAP (with the *DAH* gene inserted into the MscI-NcoI gap of pET-22b) (Arima et al. 2011a) was used for the expression of wild-type (WT) DAH and as a template for mutagenesis.

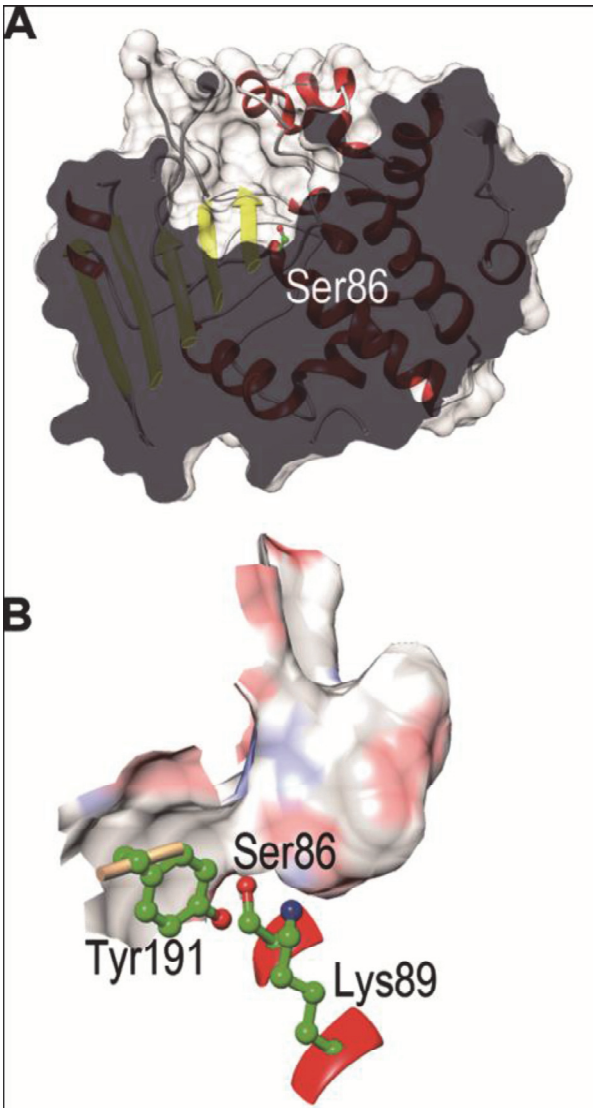

Fig. 3.1 Cavity and pocket in DAH. (A) A cross-sectional view of the molecular surface of DAH. Ribbon models: α-helices and β sheets are red and yellow, respectively. The active site Ser86 is shown as a ball and stick model colored according to atom type. The surface of the enzyme is colored light gray. (B) Shape of the pocket in DAH. Active site residues Ser86, Lys89, and Tyr191 are shown as ball and stick models colored according to atom type.

3.2.2 Structural model of mutant DAHs

The sequences of the mutant DAHs were aligned with the WT sequence (Protein Data Bank accession no. 3WWX). The alignment data were submitted to SWISS-MODEL (Arnold et al. 2006b; Biasini et al. 2014a) to generate a homology model of the mutant DAHs based on the WT template structure and the obtained structural models were analyzed using UCSF CHIMERA software (Pettersen et al. 2004). The wild-type crystal structure predicted the structure of mutants and superimposed structure were visualized by using UCSF CHIMERA software. The reference template was DAH (PDB: 3WWX) which aligned with DAA (PDB: 2DNS) structure.

3.2.3 Mutagenesis

Site-directed mutagenesis for the construction of the mutant enzymes was conducted by inverse PCR using two pairs of primers containing a point mutation (Table S1). The PCR program comprised of 18 cycles for 1 min at 95 °C, 1 min at 63 °C, and 8 min at 68 °C. The PCR product was treated with Dpn I at 37 °C overnight and then transfected into competent *E. coli* JM109 cells according to the manufacturer's protocol. The plasmid was extracted and accurate cloning was confirmed by sequencing.

3.2.4 Expression and purification of WT and mutant DAHs

E. coli Rosetta (DE3) harboring pET-82F2DAP or the expression vector for mutant DAH production was cultivated at 25 °C for 48 h in Overnight Expression Instant TB medium (50 mL; Novagen Inc., Madison, WI, USA). The culture was centrifuged to remove the cells and the recombinant enzyme was purified as previously described in (Arima et al. 2016). The culture

supernatant was concentrated to more than 10 mg·mL^{-1} with a centrifugal filter (Amicon Ultra; Millipore Corp., Billerica, MA, USA) and then dialyzed against 20 mM sodium citrate (pH 5.5). The dialysate was loaded onto a Vivapure-S spin column (Sartorius, Gottingen, Germany) equilibrated with 20 mM sodium citrate (pH 5.5). After washing the spin column with sodium citrate buffer containing 0.1 M NaCl, the bound protein was eluted with sodium citrate buffer containing 0.4 M NaCl and the active fractions were collected. The protein concentration was determined with a protein assay kit (Bio-Rad Laboratories Inc., Berkeley, CA) using bovine serum albumin as a standard. The homogeneity of the purified proteins was confirmed by 12% sodium dodecyl sulfate-polyacrylamide gel electrophoresis (SDS-PAGE) under denaturing conditions.

3.2.5 Methanol release assay

The concentration of liberated methanol is equivalent to the amount of acyl-enzyme intermediate formed in the first step of the catalytic reaction and was measured by the 4-aminoantipyrine phenol method (Allain et al. 1974) coupled with an alcohol oxidase reaction. The DAH reaction was set to 2 min for accurate measurement of initial reaction velocity and to equalize the condition of the aminolysis reaction. In 96 well microplates, DAH reaction mixtures were prepared as follows. First, 5 □L of 0.05–0.2 mg·mL^{-1} WT or mutant DAH solution was added to 40 μL of 0.5 M Tris-HCl (pH 8.5). The reaction was initiated by the addition of 5 μL of substrate (ca. 0.5 M) dissolved in dimethyl sulfoxide, continued at 25°C for 2 min, and then terminated by the addition of 50 μL of 1 M HCl. Next, 10 μL of reaction mixture was added to 90 μL of a mixture comprising 140 mM Tris-HCl (pH 8.0), 0.5 mM 4-aminoantipyrine, 2 mM phenol, 0.1 mg·mL^{-1} horseradish peroxidase, and 0.1 mg·mL^{-1} alcohol oxidase. After incubation for 30 min

at room temperature, the absorbance at 490 nm was determined by a microtiter plate reader (680; Bio-Rad Laboratories Inc.). The concentration of liberated methanol was measured from the linear part of the optical density profile of standard methanol using the same instrument.

3.2.6Assay of aminolysis and hydrolysis activity

Aminolysis and hydrolysis reactions are competitive and hydrolysis tends to occur at high temperatures; thus, the reaction was conducted to suppress hydrolysis. The activity of the aminolysis was assayed as previously described by (Elyas et al. 2018). First, 5 µL of 0.1 $mg \cdot mL^{-1}$ enzyme solution was added to 40 µL of the mixture containing 35 µL of 0.5 M Tris-HCl (pH 8.5) and 5 µL of 0.5 M 1,8-DAO. The reaction was initiated by adding 5 µL of 0.5 M Ac-Phe-OMe dissolved in dimethyl sulfoxide. The reaction was then continued at 25 °C for 2 min, and terminated by adding 50 µL 0.5 M HCl to the mixture. The reaction mixture was then analyzed by measuring the released methanol and the reaction product by using mass spectrometry (MS).

3.2.7 MS analysis

The molecular masses of the products of DAH catalytic activity were determined via electrospray ionization–time-of-flight (ESI–TOF) MS. For ESI-TOF MS analysis, the reaction mixture was diluted with a 100-fold volume of 0.1% formic acid. After the solution was filtered, 5 µL from each sample was analyzed by using an ESI-TOF MS system (LCT Premier XE or Quattro Micro API; Waters Corp.). The data were processed using a computer program (MassLynx; Waters Corp.).

Table 3.1 Sequences of mutagenesis primers used for site-directed mutagenesis.

Mutations	Primer name	Sequence (5′ to 3′)	T_m (°C)
T145F	DAH T145F_F	ATCTACAGCTACTTTGAGGACCCCGCCTT	64
	DAH T145F_R	AAGGCGGGGTCCTCAAAGTAGCTGTAGAT	64
A267V	DAH A267V_F	TCAACCCGAGCATCGTGGGCGCGGCGGG	72
	DAH A267V_R	CCCGCCGCGCCCACGATGCTCGGGTTGA	72
A267F	DAH A267F_F	TCAACCCGAGCATCTTTGGCGCGGCGGG	70
	DAH A267F_R	CCCGCCGCGCCAAAGATGCTCGGGTTGA	70
A267W	DAH A267W_F	CCCGAGCATCTGGGGCGCGGCGG	69
	DAH A267W_R	CCGCCGCGCCCCAGATGCTCGGG	69
G271F	DAH G271F_F	GGGCGCGGCGTTTGAGATGATCTCC	65
	DAH G271R_R	GGAGATCATCTCAAACGCCGCGCCC	65

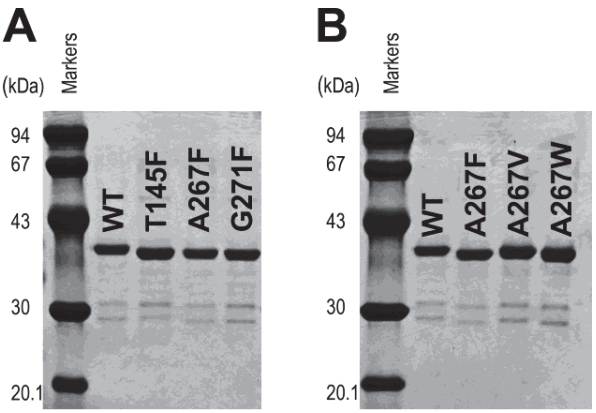

Fig. 3.2 SDS-PAGE of partially purified wild-type (WT) and mutant D-stereospecific amidohydrolases (DAHs). (A) SDS-PAGE of WT, T145F, A267F, and G271 DAHs. (B) SDS-PAGE of WT, A267F, A267V, and A267W DAHs. Samples (3 μg) were loaded on a 12% gel.

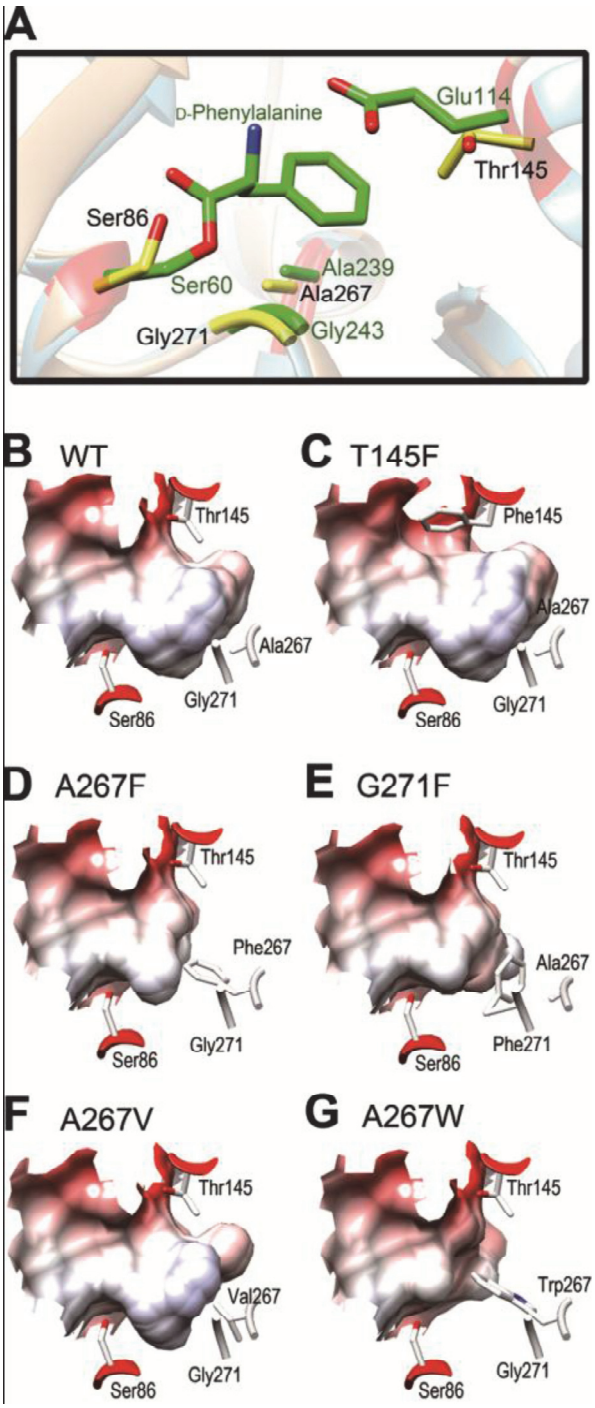

Fig. 3.3 Comparison of the local structures of DAH and DAA (A) and pocket shapes of WT DAH and the predicted structures of the mutants (B–G). (A) View of the active site of DAH superimposed on that of DAA. The DAH residues are shown as yellow sticks and those of DAA

and bound D-phenylalanine are shown as green sticks. (B–G) The model structure of DAH and the predicted structures of the mutants are superimposed on the model structure of WT DAH as viewed from the rear and at the same angle. The residues Thr145 of WT and Phe145 of T145F are shown as green sticks. The residues Ala267 of WT, Phe267 of A267F, Val267 of A267V, and Trp267 of A267W are shown as yellow sticks. The residue Phe271 of G271F is shown as cyan sticks.

3.3. RESULTS

3.3.1 Effect of Phe-substitution on acyl-enzyme intermediate formation activity

Ala-substitution is usually performed for the functional analysis of amino acid residues using mutations (Morrison and Weiss 2001) but the selected residues Thr145, Ala267, and Gly271 are small and one is Ala. We, therefore, performed Phe-substitution instead of Ala to examine the size/shape changes in the active site pocket of DAH of each mutation and its effect on the recognition of hydrophobic substrate and on stereoselectivity. Structure prediction revealed that the shape and size of the pocket was dramatically changed by mutating any one of these three residues to Phe (Fig.3.3 3.3B-3.3E) and thus we constructed the T145F, A267F, and G271F DAH variants. SDS-PAGE indicated that all the mutants could be partially purified using the method described in the Materials and Methods (Fig. 3.2). We evaluated the effect of each mutation on stereoselectivity using the free and acetylated forms of D/L-Phe-OMes as model substrates based on their previous use as model acyl-donor substrates for the aminolysis reaction of DAH used to synthesize dipeptides with a DL-configuration (Arima et al. 2011b).

The acyl-enzyme intermediate formation is the first step of the enzyme reaction (Fig.3.4) and was measured for the WT and mutant DAHs using the free and acetylated forms of D/L-Phe-OMes by the methanol release assay. WT DAH exhibited high activity toward D-Phe-OMe whereas its activity was less than half that toward L-Phe-OMe (Fig. 3.5 A), in agreement with a previous report (Arima et al. 2011b). The effect of mutations were found to vary along the aromatic substrates, this effect is not accounted for steric hindrance rather than the change of pocket hydrophobicity, In contrast, similar values were observed for the activity of WT toward acetylated D/L-Phe-OMe (Fig. 3.5 B). The mutations resulted in differences in their stereoselectivities compared with WT. For example, Thr145 is believed to supply the negative charge required for recognition of the amino group of a substrate, yet this mutation had little effect on its stereoselectivity toward both the free and acetylated forms of D/L-Phe-OMes (Fig. 3.5). In contrast, the mutation of Ala267 and Gly271, located at the bottom of the hydrophobic pocket, decreased the reaction rate toward the D- and L-configurations of the free-form substrates (Fig. 3.5 A). Furthermore, the mutant enzymes showed altered activities toward the acetylated substrates compared with their activities toward free D/L-Phe-OMes. That is, A267F exhibited an approximately two-fold higher reaction rate for Ac-D-Phe-OMe than that for Ac-L-Phe-OMe whereas the ratio of reaction rates between Ac-D-Phe-OM to Ac-L-Phe-OMe in T145F was similar to that of G271F (i. e., no significant difference in the recognition between D and L acetylated form of substrate either in T145F or in G271F mutant) (Fig. 3.5B).

3.3.2 Effect of the Ala267 mutation on acyl-enzyme intermediate formation activity

A267F and G271F were found to have different substrate specificities compared with WT DAH, with A267F showing over double the activity toward Ac-D-Phe-OMe compared with Ac-L-Phe-OMe whereas WT exhibited no significant difference in activity toward the acetylated forms of D/L-Phe-OMes. To gain deeper insight into the relationship between size/shape/hydropathy of the pocket and substrate recognition, we focused on Ala267 and substituted Ala with Trp (A267W), the bulkiest residue, and Val (A267V), a more hydrophobic residue than Ala or Phe (Kyte and Doolittle 1982). The predicted pocket structures of A267V and A267W DAH revealed different shapes, sizes, and hydrophobicities from WT DAH (Fig. 3.3F and 3.3G), and SDS-PAGE showed that both mutants could be partially purified using the method described in the Materials and Methods (Fig. 3.2).

As shown in Fig. 3.5, the A267Vand A267W mutants exhibited lower activities toward all substrates than those exhibited by WT and the other mutant DAHs. Although the mutation of Ala267 to Val or Trp remarkably decreased specific activity, the activity ratios of A267V and A267W DAHs toward the D- and L-form substrates were very similar to that of the A267F mutant. Specifically, the reaction rates of A267V and A267W DAH for D-Phe-OMe were almost the same as those for L-Phe-OMe, and the mutants exhibited around two-fold higher activity for Ac-D-Phe-OMe than that for Ac-L-Phe-OMe.

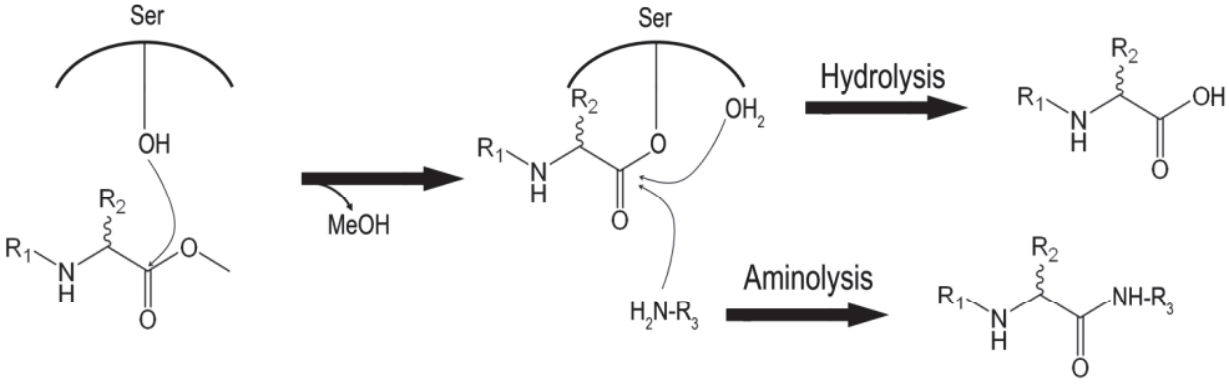

Fig. 3.4 Reaction scheme of the DAH reaction toward aminoacyl derivatives.

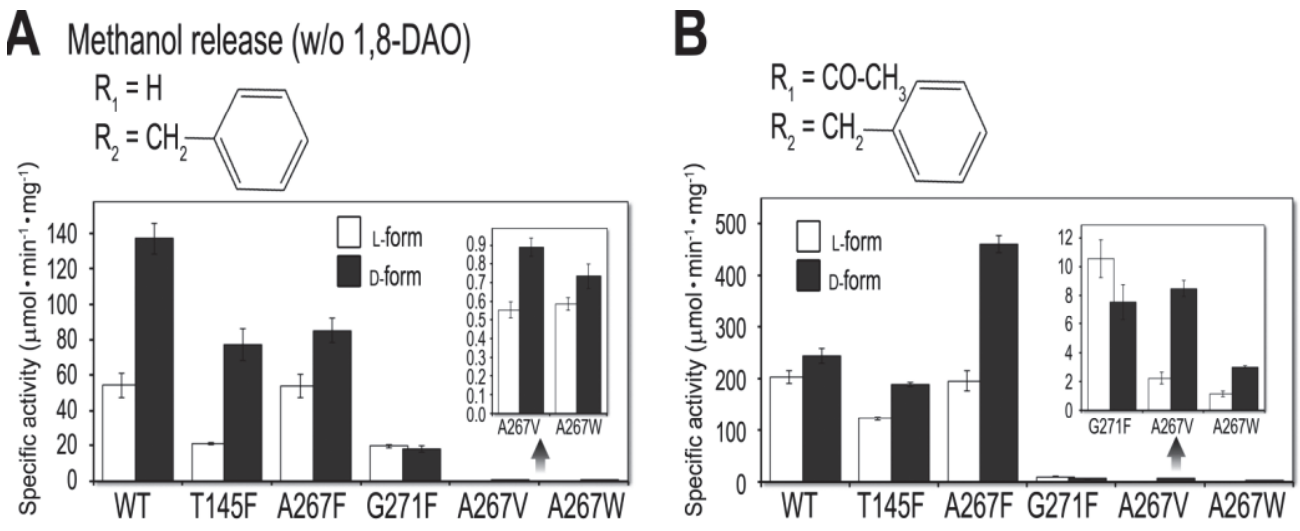

Fig. 3.5 Effect of mutation on methanol release. (A) Methanol release by the WT and mutant DAHs using D/L-Phe-OMe as substrate. Methanol is a product of the formation of the acyl-enzyme intermediate. (B) Methanol release by the WT and mutant DAHs using Ac-D/L-Phe-OMe as substrate. In both panels, the values were calculated from the specific activity of methanol production after 2-min enzyme reactions. The structures of the substrates, R_n corresponding to the scheme in Fig. 2, indicate on the respective graphs. The reactions were performed in solutions containing 50 mM substrate at pH 8.5 and 25 °C. Each value represents the mean ± SD of values from four independent experiments.

3.3.3 Kinetic analysis of the WT and mutant DAHs

The kinetic parameters of the WT and mutant DAHs toward the free and acetylated forms of D/L-Phe-OMes are shown in Table 3.2 and show that WT DAH has higher affinity for D-form substrates than for L-form substrates (K_m values are 203, 103, 103, 10.6 mM for L-Phe-OMe, D-Phe-OMe, Ac-L-Phe-OMe, and Ac-D-Phe-OMe, respectively). Acetylated substrates were considered appropriate for catalysis by DAH because the k_{cat}/K_m values for the acetylated forms of the substrates (k_{cat}/K_m for Ac-L-Phe-OMe and Ac-D-Phe-OMe are 5.02 and 15.3 s^{-1}, respectively) are higher than those for the free forms (k_{cat}/K_m for L-Phe-OMe and D-Phe-OMe are 1.23 and 3.08 s^{-1}, respectively). The mutation of Ala267 to Phe decreased the K_m values for all substrates (Table 3.2), suggesting that the addition of a phenyl ring at the Ala267 position increased the affinity of the binding pocket to the substrate's benzene ring. In addition, similar to the specific activities shown in Fig. 3.5 B, this mutation also increased k_{cat} and catalytic efficiency (k_{cat}/K_m) toward Ac-D-Phe-OMe, indicating that this mutation affects positively the acyl-enzyme intermediate formation reaction with Ac-D-Phe-OMe.

In contrast to the mutation of Ala267 to Phe, the Val and Trp mutations negatively affected acyl-enzyme intermediate formation activity. The very high K_m values of A267V and A267W for L-Phe-OMe and Ac-L-Phe-OMe prevented estimation of the kinetic parameters of both substrates. However, both mutations resulted in increased K_m values for all substrates (Table 3.2), indicating a weakened affinity for all substrates. Similar to the specific activity results shown in Fig. 3.5B, the catalytic efficiencies (k_{cat}/K_m) toward both D-Phe-OMe and Ac-D-Phe-OMe were dramatically decreased by the mutation of Ala267 to Val or Trp (Table 3.2). A similar effect of the mutation of Gly271 to Phe on enzyme kinetics was observed (Table 3.2) and

thus substrate binding by DAH is likely disrupted by modifications to the structure and hydrophobicity of the bottom of the active site pocket. Furthermore, the effect of the mutation of Thr145 to Phe was observed in the k_{cat} for acetylated substrate rather than in the K_m value (Table 3.2). Thr145 had been believed to be involved in the stereospecific recognition of the amino group of the substrate but our results suggest that it is involved in a catalytic turnover rather than in D-/L- recognition by DAH.

3.3.4 Effect of Mutations on Aminolysis Activity

As mentioned in the Introduction, DAH exhibits high aminolysis activity as a side reaction in accordance with its hydrolysis activity. We examined the acyl-enzyme intermediate formation, hydrolysis, and aminolysis activities of the WT and mutant DAHs by using the acetylated form of Phe-OMe as an acyl-donor and 1,8-DAO as an acyl-acceptor at pH 8.5, 4 °C, for 2 min. The trends in the effects of mutation on all activities (methanol release, hydrolysis, and aminolysis) were similar to the above investigations using a single substrate (Fig. 3.6), but the activity of A267F to Ac-D- Phe-OMe was significantly higher than that of the other mutations. Furthermore, mutation of Gly271 drastically decreased aminolysis activity toward both substrates (Ac-D/L-Phe-OMe) (Fig. 3.6).

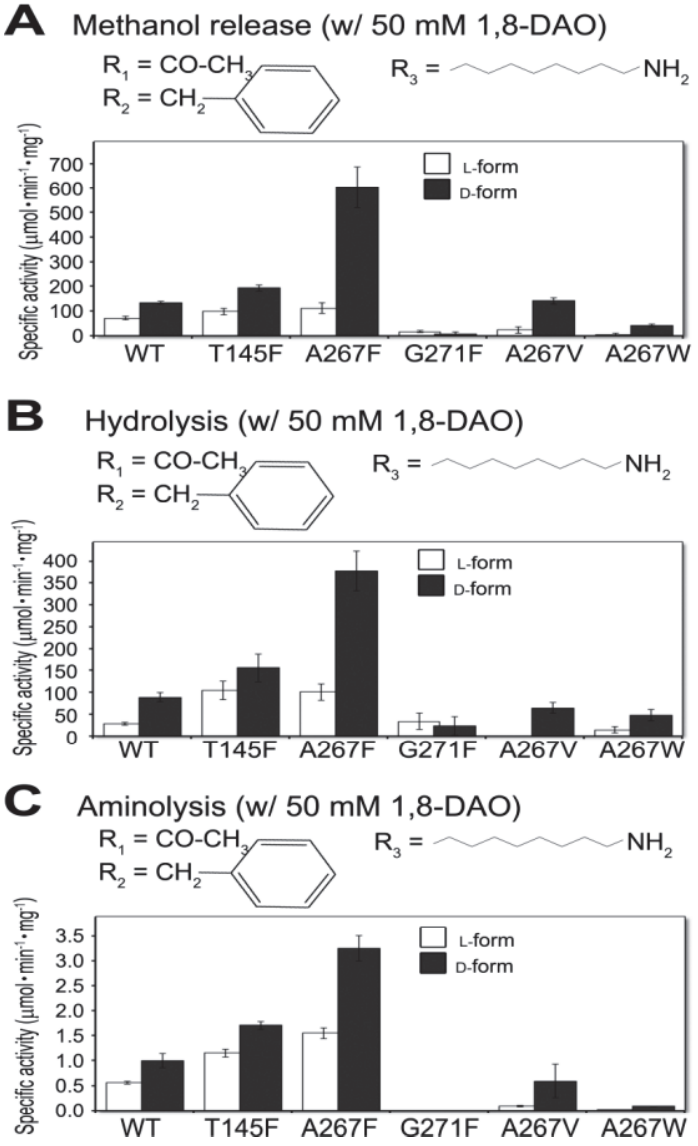

Fig. 3.6 Effect of mutation on methanol release, hydrolysis, and aminolysis activities in the presence of 50 mM 1,8-DAO as acyl acceptor. (A) Methanol release by the WT and mutant DAHs using D/L-Phe-OMe as substrate. Methanol is a product of the formation of the acyl-enzyme intermediate. (B) Hydrolysis by the WT and mutant DAHs using Ac-D/L-Phe-OMe as substrate. The values of specific activities were determined by measuring the concentration of liberated Ac-Phe after 2 min enzyme reaction by using ESI-MS. (C) Aminolysis by the WT and mutant DAHs using Ac-D/L-Phe-OMe as substrate. The values of relative activities were determined by measuring the relative concentration of produced Ac-Phe-1,8-DAO after 2 min enzyme reaction by using ESI-MS. The structures of the substrates, R_n corresponding to the scheme in Fig. 2, indicate on the respective graphs. Each value represents the mean ± SD of values from four independent experiments.

Table 3.2. Enzyme kinetics for acyl-enzyme intermediate formation (methanol release). Reactions were performed at pH 8.5 for 2 min. Values are calculated from a nonlinear regression fit to the Michaelis–Menten equation using initial estimates from double-reciprocal plots (1/S vs. 1/V). The values are expressed as the mean ± SD of four independent experiments.

DAH variant	L-Phe-OMe			D-Phe-OMe			Ac-L-Phe-OMe			Ac-D-Phe-OMe		
	k_{cat} (s^{-1})	K_m (mM)	k_{cat}/K_m ($s^{-1}\cdot mM^{-1}$)	k_{cat} (s^{-1})	K_m (mM)	k_{cat}/K_m ($s^{-1}\cdot mM^{-1}$)	k_{cat} (s^{-1})	K_m (mM)	k_{cat}/K_m ($s^{-1}\cdot mM^{-1}$)	k_{cat} (s^{-1})	K_m (mM)	k_{cat}/K_m ($s^{-1}\cdot mM^{-1}$)
WT	250[a] ± 44	203[a] ± 61	1.23	317[a] ± 44	103[a] ± 21	3.08	620[a] ± 51	103[a] ± 15	5.02	162 ± 27	10.6 ± 3.2	15.3
A267F	199[a] ± 19	162[a] ± 20	1.23	181 ± 46	67.1 ± 27.3	2.70	284 ± 12	46.8 ± 9.8	5.07	313 ± 15	11.1 ± 1.1	28.2
A267V	n.d.[b]	n.d.[b]	n.d.[b]	95.9[a] ± 26.9	142[a] ± 22	1.35	n.d.[b]	n.d.[b]	n.d.[b]	535[a] ± 124	334[a] ± 60	1.60
A267W	n.d.[b]	n.d.[b]	n.d.[b]	86.5[a] ± 19.9	127[a] ± 38	1.37	n.d.[b]	n.d.[b]	n.d.[b]	21.9 ± 5.1	20.7 ± 3.9	1.06
T145F	n.d.[b]	n.d.[b]	n.d.[b]	256[a] ± 60	196[a] ± 70	1.31	108 ± 8	43.8 ± 4.7	2.47	77.5 ± 2.7	12,4 ± 1.1	6.25
G271F	n.d.[b]	n.d.[b]	n.d.[b]	184[a] ± 50	638[a] ± 211	0.29	122[a] ± 28	454[a] ± 115	0.29	34.6[a] ± 4.2	114[a] ± 32	0.30

[a] Apparent values because substrates at concentrations over 100 mM could not be dissolved in pH 8.5 water. The values were calculated from nonlinear regression fitting to the Michaelis–Menten equation using initial estimates from double-reciprocal plots (1/S vs. 1/V)

[b] n.d.: not determined due to high K_m values.

3.4 DISCUSSION

We previously solved the crystal structures of DAH complexed with 1,8-diaminooctane (Arima et al. 2016) and observed that DAH possesses a small pocket in the vicinity of the active site Ser86. Functional analysis of residues comprising the active site pocket should provide insights into the catalytic mechanism, including substrate recognition. As mentioned in the Introduction, the DAA crystal structure indicates that the three residues Glu114, Ala239, and Gly243 are involved in D-phenylalanine recognition, and these residues correspond to Thr145, Ala267, and Gly271 in DAH (Okazaki et al. 2007). In the present study, we performed a site-directed mutagenesis analysis of these residues in DAH to investigate how structural factors correlate to the recognition of hydrophobic substrates. The structural and mechanistic factors influence the stereoselective recognition has subjected to intensive research (Kyte and Doolittle 1982; Andrew D. Mesecar 2000; Wombacher et al. 2006; Okazaki et al. 2008b). However, enzyme engineering (e.g. site-directed mutagenesis) and *in vitro* evolution aid in understanding the structural basis of stereoselectivity and also provide tools to manipulate this property (Wombacher et al. 2006)

The superimposition data constructed with local structure of DAH and bound D-phenylalanine in DAA shows the reasonable distances between D-phenylalanine and residues focused in this study (Fig. 3.7A). The space of the active site pocket of DAH is wide enough to bind with D-phenylalanine. The structure and electrostatic environment of the active site pocket of DAH should be dramatically changed by mutation, with the pocket spaces in the predicted structures of A267F, A267V, A267W, and G271F DAHs being narrower than that of WT (Fig. 3.3B, 3.3D–3.3G). Such drastic modifications of the pocket structure would likely significantly reduce the catalytic ability and indeed a significant reduction in catalytic ability was observed by the mutation of Gly271 to Phe and Ala267 to Val or Trp. In fact, the superimpositions data

constructed with local structure of the above mutant DAHs and bound D-phenylalanine in DAA contain structurally impossible parts (Fig. 3.7D–3.7F), and thus, the confirmation of the bound -

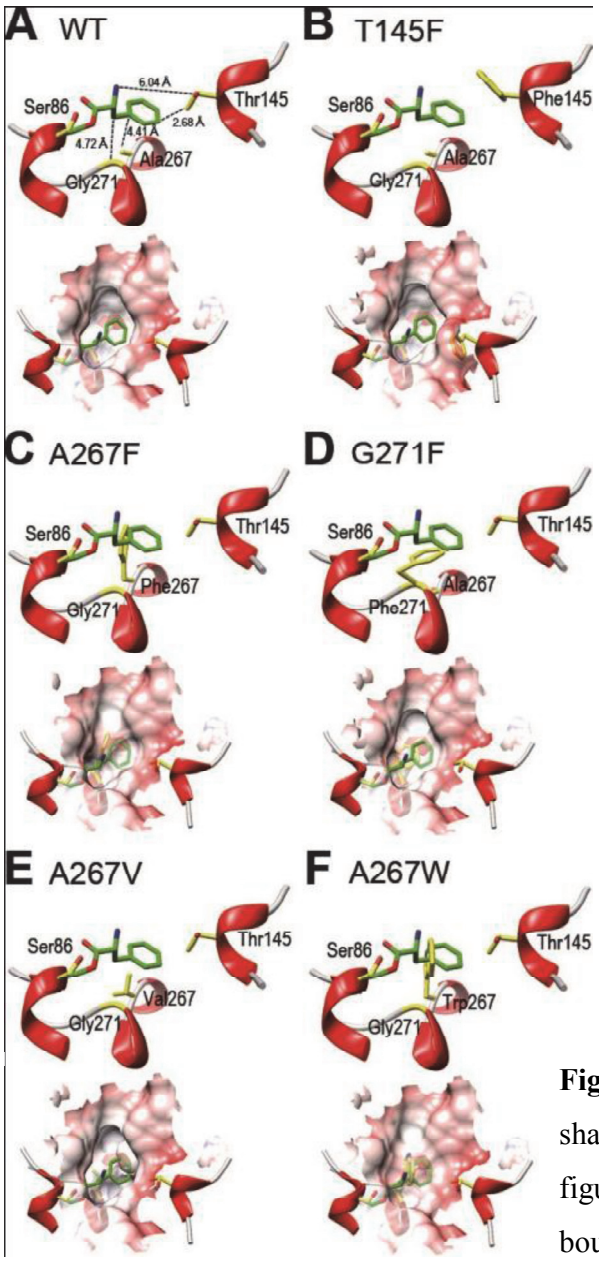

Fig. 3.7 Local structures (upper panel) and predicted pocket shapes (lower panel) of WT (A) and mutant (B–F) DAHs. All figures were constructed by superimposition with DAA, and bound D-phenylalanine in DAA structure is shown as green sticks. The DAH residues are shown as yellow sticks. The pocket structure of DAH and the predicted pocket structures of the mutants are shown as viewed from the upper and at the same angle.

substrate in mutant DAHs was considered to be different from that in WT DAH. In contrast, the substitution of Ala267 to Phe resulted in enhanced catalytic efficiency for Ac-D-Phe-OMe rather than loss of activity, clearly demonstrating that shape, electrostatic environment, and the space around the bottom of the hydrophobic pocket are all involved in the recognition of hydrophobic substrates. Specifically, A267F DAH accepted the acetylated form of D-Phe-OMe as a preferred substrate for acyl-enzyme intermediate formation, hydrolysis, and aminolysis reaction (Fig. 3.5, Table 3.2), suggesting an interaction between the benzene ring of the substrate and that of the Phe side chain in A267F DAH during the catalytic reaction. In the superimposition data constructed with local structure of A267F DAH and bound D-phenylalanine in DAA, the distance between the phenyl ring of position at 267 and the substrate is too close (less than 1 Å, Fig.3.7 C). This model is an impossible structure, and the confirmation of the bound substrate in A267F DAH is different from that in WT DAH. The binding manner of the substrate before the nucleophilic attack by hydroxyl group of Ser86 also was considered to be changed by the mutation. Because the mutation of Ala267 to Phe resulted in enhanced catalytic efficiency for Ac-D-Phe-OMe, the substrate binding manner of A267F DAH is presumed to be a conformation susceptible to nucleophilic attack by hydroxyl group of Ser86.

The ratios of the specific activities of T145F between the D- and L- form substrates were almost identical to those of WT, showing that the mutation of Thr145 to Phe had little effect on the stereoselectivity of the enzyme toward both the free and acetylated forms of D/L-Phe-OMes (Fig. 3.5). This result suggests that Thr145 is involved in the recognition of substrate using properties other than stereoselectivity. The long distance between the hydroxyl group of Thr145 and amino group of D-phenylalanine (approximately 6 Å, Fig. 3.7A, 3.7B) supports the above hypothesis. In contrast, the mutation of Gly271 to Phe apparently affects the stereoselectivity of

DAH; the specific activities of G271F toward L-Phe-OMe and Ac-L-Phe-OMe were higher than those toward D-Phe-OMe and Ac-D-Phe-OMe, respectively. The differences in specific activities and kinetic values between the D- and L- form substrates were similar within the margins of experimental error and thus we could not conclude that Gly271 is involved in the recognition of D- and L- form substrates. Many questions regarding the substrate selectivity of DAH (and this class of enzymes) remain unanswered and thus further detailed studies are required to clarify the reaction mechanism in terms of substrate recognition.

3.5 CONCLUSION

In this study, we attempted to analyze the structural factors of the DAH binding pocket that affect the recognition of both hydrophobic substrates and the stereoselectivity of the substrate. To this end, we conducted a mutagenesis assay for the formation of acyl-enzyme intermediates and aminolysis. The results revealed that the residues located at the bottom of the pocket play an important role in the recognition of hydrophobic substrates. Ala267 and Gly271 form the bottom of the hydrophobic active site pocket of DAH and their substitution affected enzyme activity toward hydrophobic substrates, thereby identifying Ala 267 and Gly271 as key positions for the selectivity of hydrophobic substrates. The substitution of Ala267 to Phe reduced the K_m values for all substrates except Ac-D-Phe-OMe. The present structure/function relationship findings deepen our understanding of the catalytic mechanism of serine peptidases.

CHAPTER FOUR

ENHANCEMENT OF AMINOLYSIS ACTIVITY BY SPACE FILLING OF ACTIVE SITE POCKET OF D-STEREOSPECIFIC AMIDOHYDROLASE

4.1. INTRODUCTION

Serine peptidases function in a wide range of physiological processes, such as digestion, protein maturation and turnover, homeostasis, and immune responses (Hedstrom 2002a; Page and Di Cera 2008; Ekici et al. 2008; Zakharova et al. 2009). The catalytic mechanism of serine peptidases appears to be conserved among the members of this extensive family. First, a covalent acyl-enzyme intermediate is generated with a substrate that is an acyl donor. Next, the intermediate undergoes nucleophilic attack by water (Fig. 4.1). Meanwhile, in the later step, nucleophilic attack by an amino group instead of a water molecule occurs and forms an amide bond (Fig. 4. 1) (Yokozeki and Hara 2005; Zakharova et al. 2009). The reaction is termed "aminolysis" and observed in the presence of relatively high concentrations of primary amine, which are not achieved under physiological conditions. In this reaction, primary amine acts as an acyl acceptor. In an organism, the main function of serine peptidase is probably hydrolysis, unexpected functions such as aminolysis are often observed under artificial conditions (Bordusa 2002; Yazawa and Numata 2014; Goswami and Van Lanen 2015). Because amino acids can act as acyl acceptors, the unnatural aminolysis reaction of serine peptidases has attracted attention as a method to synthesize various peptides that cannot be produced under natural conditions.

The D-stereospecific amidohydrolase from *Streptomyces* sp. 82F2 (DAH) is a serine peptidase belonging to family S12 in MEROPS (Arima et al. 2011a, b, 2016) and recognizes D-amino acyl derivatives mainly as acyl donor substrates (Arima et al. 2011a). The enzyme exhibits high aminolysis activity and mainly recognizes L-amino acids and their derivatives as

acyl acceptors, making this enzyme of particular interest for synthesizing dipeptides with a DL-configuration (Arima et al. 2011b). Indeed, DAH has been used to synthesize the cyclic dipeptide cyclo (D-Pro-L-Arg) in a one-step/one-pot reaction (Arima et al. 2011b) as the lead compound of a pesticide which inhibits family 18 chitinases (Izumida et al. 1996; Houston et al. 2004).

Crystallographic analysis of DAH (PDB: 3WWX) revealed a large cavity that leads to the active center (Fig. 4.3A) (Arima et al. 2016). The side chains of Ser86 and Lys89 that create a catalytic Ser/Lys dyad were positioned at the center of the large cavity. Tyr191, which is close to the Ser/Lys dyad, acts as the general base to activate Ser as a nucleophile for the acyl donor during the acylation step and the water molecule during hydrolysis. In addition, there is a pocket near the active center residues Ser86, Ly89 and Tyr191 (Fig. 4.3A). This pocket plays functional roles in substrate recognition and aminolysis activity (Arima et al. 2016; Elyas et al. 2018). Therefore, an investigation into the effects of modification of the active site pocket on the aminolysis activity of DAH provides important information for the rational modification of enzymes aimed to develop a convenient biocatalyst for peptide synthesis.

The active site pocket of DAH is considered to accommodate acyl donor or acyl acceptor substrate. Ala267 and Gly271 are located at the bottom of the hydrophobic pocket (Fig. 4.3A). Specifically, the shape and electrostatic environment of the pocket are likely related to substrate preference (Arima et al. 2016; Elyas et al. 2018). Our previous report indicated that the expanding the space of DAH active site pocket led to change in substrate specificity in aminolysis activity (Elyas et al. 2018). The present study aimed to investigate the relationship between active site pocket and aminolysis activity from an opposite approach to our previous study. We focused on Ala267 and Gly271 in DAH for assessing the effect of space filling of the

active site pocket on its aminolysis activity. The residues were replaced with the bulky amino acid residue Phe to fill the space of active site pocket, and then we evaluated the effect of space modification on the ability of the enzyme to form acyl-enzyme intermediates, hydrolysis, and aminolysis. We found that substitution of position 267 with the bulky residue, Phe, enhances the enzyme's aminolysis catalysis. Moreover, the same effect of the mutation was observed in the efficiency of the synthetic activity of biologically active cyclic dipeptide, cyclo(D-Pro-L-Arg) ($c(_{D}P\text{-}_{L}R)$).

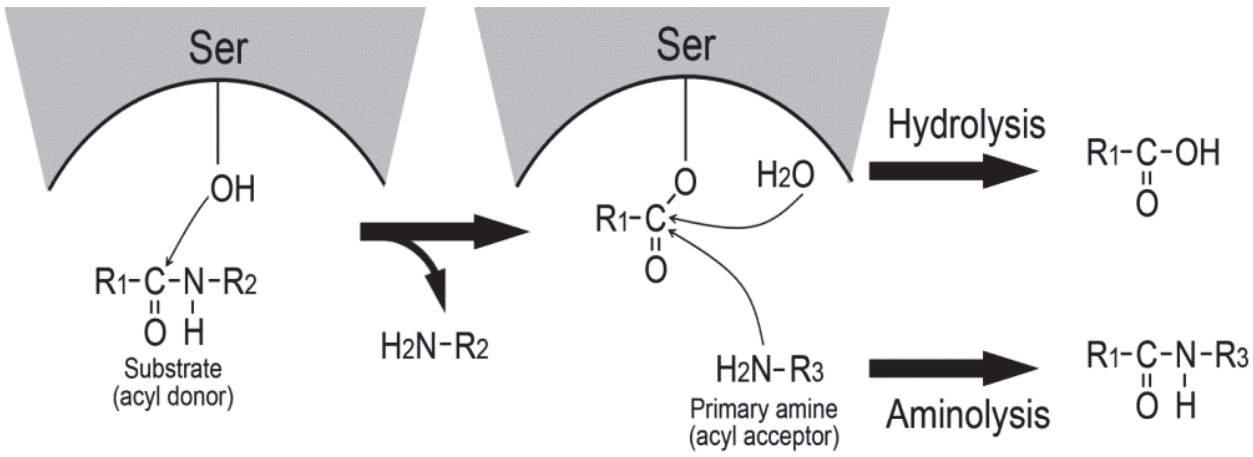

Fig. 4.1 Scheme of the hydrolysis and aminolysis reactions catalyzed by serine peptidases.

4.2MATERIALS AND METHODS

4.2.1 Materials, bacterial strains, and plasmids

Amino acids and aminoacyl ester derivatives were purchased from Bachem AG (Bubendorf, Switzerland), Aldrich Chemical Co., Inc. (Milwaukee, USA), Sigma Chemical Co. (St. Louis, MO, USA), Novabiochem Corp. (San Diego, California, USA), Wako Pure Chemical Industries Ltd. (Osaka, Japan), and Tokyo Chemical Corp. (Tokyo, Japan). *Escherichia coli* JM109 was

used as a host strain for general cloning procedures and *E. coli* Rosetta (DE3) was used as a host strain for gene expression. Plasmid pET-82F2DAP (with the DAH gene inserted into the MscI-NcoI gap of pET-22b) (Arima et al. 2011b) was used for the expression of wild-type (WT) DAH and as a template for mutagenesis.

4.2.2 Structural model of mutant DAHs

The sequences of the mutant DAHs were aligned with the WT sequence (Protein Data Bank accession no. 3WWX). The alignment data were submitted to SWISS-MODEL (Arnold et al. 2006b; Biasini et al. 2014b) to generate a homology model of the mutant DAHs based on the WT template structure and the obtained structural models were analyzed using UCSF CHIMERA software (Pettersen et al. 2004).

4.2.3 Mutagenesis

Site-directed mutagenesis for the construction of the mutant enzymes was conducted by inverse PCR using two pairs of primers containing a point mutation (Table 4.1). The PCR program comprised of 18 cycles of 1 min at 95 °C, 1 min at 63 °C, and 8 min at 68 °C. The PCR product was treated with Dpn I at 37 °C overnight and then transfected into competent *E. coli* JM109 cells according to the manufacturer's protocol. The plasmid was extracted and accurate cloning was confirmed by sequencing.

4.2.4 Expression and purification of WT and mutant DAHs

E. coli Rosetta (DE3) harboring pET-82F2DAP or the expression vector for mutant DAH production was cultivated at 25 °C for 48 h in Overnight Expression Instant TB medium (50 mL;

Novagen Inc., Madison, WI, USA). The culture was centrifuged to remove the cells and the recombinant enzyme was purified as follows. The culture supernatant was concentrated to more than 10 mg·mL^{-1} with a centrifugal filter (Amicon Ultra; Millipore Corp., Billerica, MA, USA) and then dialyzed against 20 mM sodium citrate (pH 5.5). The dialysate was loaded onto a Vivapure-S spin column (Sartorius, Gottingen, Germany) equilibrated with 20 mM sodium citrate (pH 5.5). After washing the spin column with sodium citrate buffer containing 0.1 M NaCl, the bound protein was eluted with sodium citrate buffer containing 0.4 M NaCl and the active fractions were collected. The protein concentration was determined with a protein assay kit (Bio-Rad Laboratories Inc., Berkeley, CA) using bovine serum albumin as a standard. The homogeneity of the purified proteins was confirmed by 12% sodium dodecyl sulfate-polyacrylamide gel electrophoresis (SDS-PAGE) under denaturing conditions(Laemmli 1970).

4.2.5 Enzyme reaction

Aminolysis and hydrolysis reactions are competitive and hydrolysis tends to occur at high temperatures; thus, the reaction was conducted at 4 °C to suppress hydrolysis. In addition, pH 8.5 was adopted for the aminolysis reaction to avoid the non-enzymatic degradation of ester substrates. The activity of DAH was assayed as follows. First, 5 μL of 0.1 mg·mL^{-1} enzyme solution was added to 40 μL of the mixture containing 35 μL of 0.5 M Tris-HCl (pH 8.5) and 5 μL of 0.5 M acyl acceptor substrate Trp. The reaction was initiated by adding 5 μL of 0.5 M acyl donor substrate (acetylated forms of (Ac-) Phe-methyl ester (-OMe) solution dissolved in dimethyl sulfoxide). The reaction was then continued at 4 °C for 2 min. The reaction was terminated by adding 50 μL 0.5 M HCl to the mixture. The reaction mixture was then analyzed by measuring the released methanol and by using mass spectrometry (MS).

4.2.6 Methanol release assay

The concentration of liberated methanol is equivalent to the amount of acyl-enzyme intermediate formed in the first step of the catalytic reaction and was measured by the 4-aminoantipyrine phenol method (Allain et al. 1974) coupled with an alcohol oxidase reaction (Mangos and Haas 1996). 10 μL of DAH reaction mixture was added to 90 μL of a mixture comprising 140 mM Tris-HCl (pH 8.0), 0.5 mM 4-aminoantipyrine, 2 mM phenol, 0.1 $mg \cdot mL^{-1}$ horseradish peroxidase, and 0.1 $mg \cdot mL^{-1}$ alcohol oxidase. After incubation for 30 min at room temperature, the absorbance at 490 nm was determined by a microtiter plate reader (680; Bio-Rad Laboratories Inc.). The concentration of liberated methanol was measured from the linear part of the optical density profile of standard methanol using the same instrument.

4.2.7 MS analysis

The molecular masses of the products of DAH catalytic activity were determined via electrospray ionization (ESI–TOF) MS. For ESI-TOF MS analysis, the reaction mixture was diluted with a 200-fold volume of 0.1% formic acid. After the solution was filtered, 5 μL from each sample was analyzed by using an ESI-TOF MS system (LCT Premier XE or Quattro Micro API; Waters Corp.). The data were processed using a computer program (MassLynx; Waters Corp.).

4.2.8 c($_D$P-$_L$R) synthesis

The reaction was initiated by adding 5 μL of 0.1 $mg \cdot mL^{-1}$ enzyme solution to 45 μL of the mixture containing 35 μL of 0.5 M Tris-HCl (pH 8.5), 5 μL of 0.5 M D-Pro-benzyl ester (-OBzl)

dissolved in dimethyl sulfoxide and 5 μL of 0.5M L-Arg-OMe dissolved in dimethyl sulfoxide. The reaction was then continued at 4 °C for 10–1800 min. The reaction was terminated by adding 50 μL 0.5 M HCl to the mixture. The reaction mixture was then analyzed by using mass spectrometry (MS).

Table 4.1 Sequences of mutagenesis primers used for site-directed mutagenesis.

Mutations	Primer name	Sequence (5' to 3')	T_m (°C)
A267F	DAH A267F_F	TCAACCCGAGCATCTTTGGCGCGGCGGG	70
	DAH A267F_R	CCCGCCGCGCCAAAGATGCTCGGGTTGA	70
G271F	DAH G271F_F	GGGCGCGGCGTTTGAGATGATCTCC	65
	DAH G271R_R	GGAGATCATCTCAAACGCCGCGCCC	65

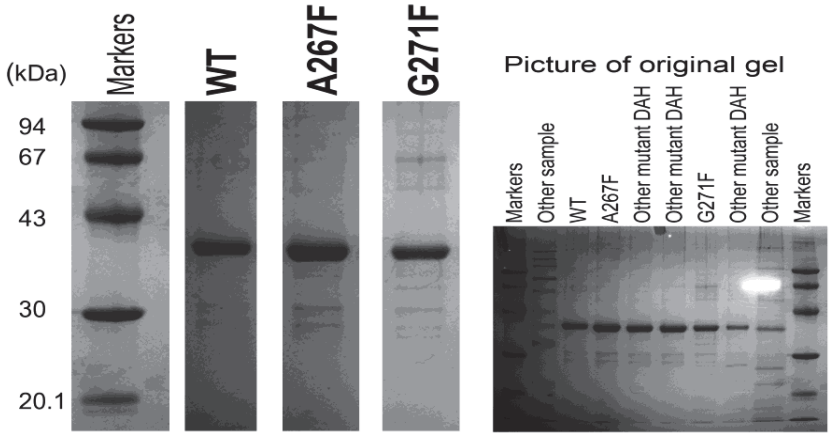

Fig.4.2 SDS-PAGE of partially purified wild-type (WT) and mutant D-stereospecific amidohydrolases (DAHs). The left panel shows the SDS-PAGE lanes for WT, A267F, and G271 DAHs. The original gel is shown in the right panel.

4.3 RESULTS

4.3.1 Effect of space filling of active site pocket on aminolysis activity

To fill the space of active site pocket of DAH, we constructed two mutant enzymes, A267F, and G271F DAHs. Structure prediction revealed that the shape and size of the pocket were dramatically changed by mutating to Phe (Fig. 4.3B). SDS-PAGE indicated that both mutants could be partially purified using the method described in the Materials and Methods (Fig. 4.2). To investigate the possible effects of mutations on aminolysis, we examined the products of the enzyme reaction by using Ac-D/L-Phe-OMe in combination with D/L-Trp as the acyl-donor and acyl-acceptor substrates, respectively, under optimum conditions for aminolysis (i.e., at 4 °C and pH 8.5).

The acyl-enzyme intermediate formation is the first step of the enzyme reaction it consider to be rate-limiting step of reaction rather than nucleophilic attack of water molecule or acyl acceptor substrate (Fig. 4.4A) and was measured by the methanol release assay. For the activities of WT, similar values were observed among the respective sets of acyl donor and acyl acceptor (Fig. 4.4B). The variants different reaction rates and stereoselectivities compared with WT. That is, mutation of Ala267 to Phe enhanced the methanol release for Ac-D-Phe-OMe by approximately three-fold whereas no enhancement was observed in the methanol release for Ac-L-Phe-OMe. In contrast to A267F DAH, G271F DAH exhibited lower activities than WT; moreover, this mutant has the same stereoselectivity as that of the wild-type. As portrayed in Fig. 4.4C and 4.4 D, the same level of Ac-D-Phe formation (hydrolysis) and a higher level of condensation production rate were observed in the A267F mutant when used L-Trp as an acyl acceptor substrate. In contrast, no enhancement of aminolysis activity was observed in the G271F mutant; rather a lack of aminolysis was observed (Fig. 4.4 D). Although the difference between actual values of relative aminolysis reaction rate and values obtained by subtracting hydrolysis from methanol release was observed, the tendency of activity rate was similar (Fig. 4.4 D). In addition to the

above results, we found that DAH strictly recognizes L-amino acids as acyl acceptor substrate rather than D-amino acids as acyl donor substrates by this investigation.

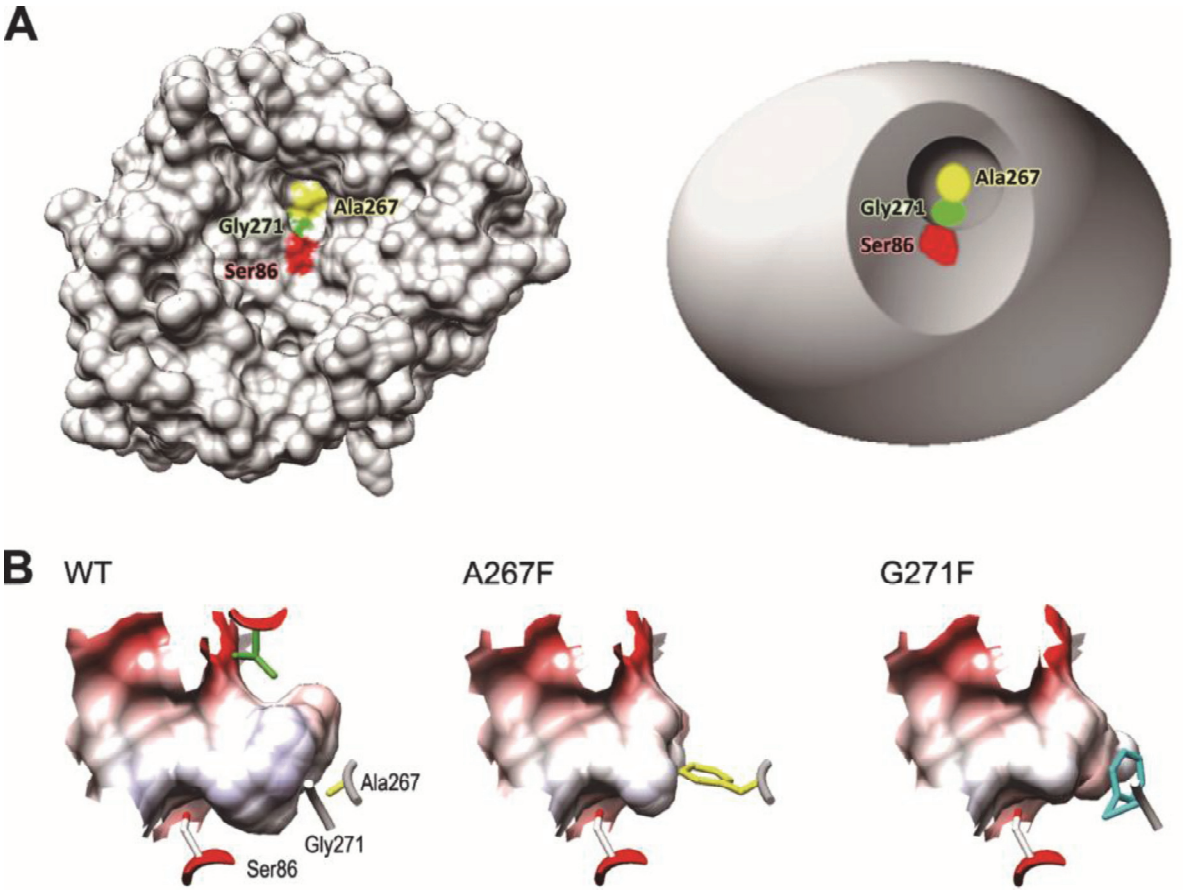

Fig. 4.3 Structure of the active site pocket of DAH. (A) The surface structure of DAH and simplified representation. The position of active site Ser86, Ala267, and Gly271 are highlighted in red, yellow, and green, respectively. (B) Pocket shapes of WT DAH and the predicted structures of the mutant DAHs. The model structure of DAH and the predicted structures of the mutants are superimposed on the model structure of WT DAH as viewed from the rear and at the same angle. The active site residue Ser86 of WT, A267F, and G271F are shown as white sticks. The residues Ala267 of WT and Phe267 of A267F are shown as yellow sticks. The residue Phe271 of G271F is shown as cyan sticks.

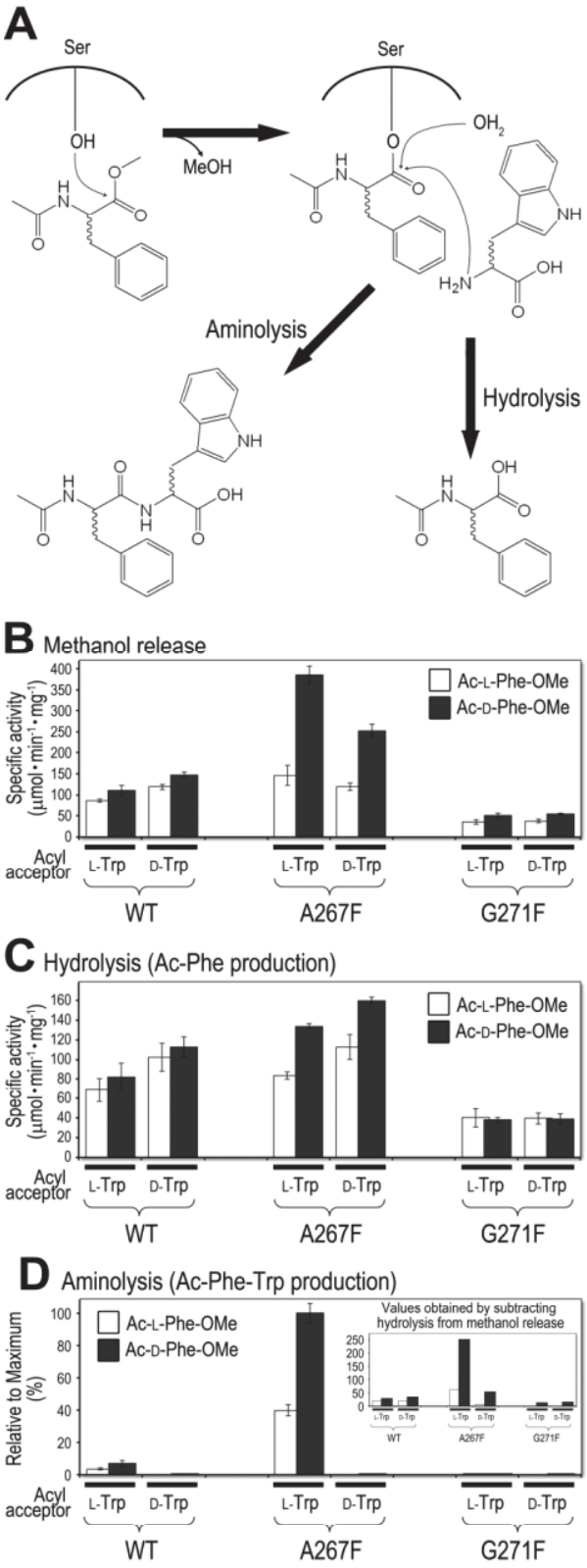

Fig. 4.4 Effect of mutation on Ac-Phe-Trp production by aminolysis function of DAH. (A) Reaction scheme of the DAH reaction for Ac-Phe-Trp production. (B) Methanol release by the WT and mutant DAHs using Ac-D/L-Phe-OMe and D/L-Trp as acyl donor and acceptor substrates, respectively. Methanol is a product of the formation of the acyl-enzyme intermediate. (C) Ac-Phe production by the WT and mutant DAHs using D/L-Phe-OMe and D/L-Trp as acyl donor and acceptor substrates, respectively. Ac-Phe is a product resulting from hydrolysis. (D) Ac-Phe-Trp production by the WT and mutant DAHs using D/L-Phe-OMe and D/L-Trp as acyl donor and acceptor substrates, respectively. Ac-Phe-Trp is a product resulting from hydrolysis. In panels (B), (C), and (D), the values were calculated from the concentration (methanol and Ac-Phe) or relative concentration (Ac-Phe-Trp) of enzyme reaction products after 2-min enzyme reactions. The reactions were performed in solutions containing 0.01 mg enzyme and 50 mM substrate at pH 8.5 and 4 °C. Each value represents the mean ± SD of values from four independent experiments.

4.3.2 Effect of space filling of active site pocket on c($_{D}$P-$_{L}$R) synthetic activity

Biologically active cyclic dipeptide, c($_{D}$P-$_{L}$R), is known to act as a specific inhibitor of family 18 chitinases and regarded as the ideal lead compound for the development of antifungal reagents and insecticide (Izumida et al. 1996; Houston et al. 2002). Our previous study demonstrated that c($_{D}$P-$_{L}$R) was successfully produced in one-pot/one-step reaction manner by the aminolysis function of DAH(Arima et al. 2011b). To confirm whether the effect of space filling of active site pocket was similar in c($_{D}$P-$_{L}$R) synthesis to the previously mentioned investigation or not, we next compared the c($_{D}$P-$_{L}$R) synthetic activity of WT and mutant DAHs. We used D-Pro-OBzl and L-Arg-OMe, as acyl donor and acceptor substrates, respectively for c($_{D}$P-$_{L}$R) synthesis in a one-pot reaction.

As presented in Fig. 4.5 A, a covalent acyl-enzyme intermediate generated from the DAH reaction with D-Pro-OBzl undergoes to nucleophilic attack by a water molecule or L-Arg-OMe. Therefore, the efficiency of c($_{D}$P-$_{L}$R) synthesis depends on the reaction rate for the nucleophilic attack by L-Arg-OMe. As portrayed in Fig. 4.5 B, the relative reaction rate of A267F DAH for D-Pro-L-Arg-OMe was significantly greater than WT and G271F DAHs. Because the same effect as Ac-Phe-Trp production was observed in this examination, the result indicates that the substitution of Ala267 with Phe enhances the nucleophilic attack by acyl acceptor substrate.

4.3.3 Time dependence on c($_{D}$P-$_{L}$R) synthesis

Finally, we evaluated time dependence on the c($_{D}$P-$_{L}$R) production by WT and mutant DAHs. The result of the investigation of time dependence shows that A267F DAH preferentially catalyzed aminolysis. The rate for D-Pro-OBzl consumption was higher in A267F than in WT and G271F (left panel in Fig. 4.5 C). In addition, significant consumption of L-Arg-OMe was

observed in only A267F DAH (second panel from the left in Fig. 4.5 C). In terms of the products, WT and G271F DAHs converted mainly from D-Pro-OBzl to D-Pro by their hydrolysis function and produced a slight amount of D-Pro-L-Arg-OMe by their aminolysis function (middle and second panel from the right in Fig. 4.5 C). In contrast, A267F DAH exhibited efficient synthesis of D-Pro-L-Arg-OMe and lower hydrolysis activity than WT and G271F DAHs. In the process for c($_{D}$P-$_{L}$R) synthesis, cyclization of D-Pro-L-Arg-OMe was occurred non-enzymatically (Fig. 4.5 A) (Arima et al. 2011b), resulting in yielding c($_{D}$P-$_{L}$R) as a final product. As portrayed in the left panel of Fig. 4.5 C, the amount of produced c($_{D}$P-$_{L}$R) by the catalysis of A267F was significantly greater than WT and A267F DAHs.

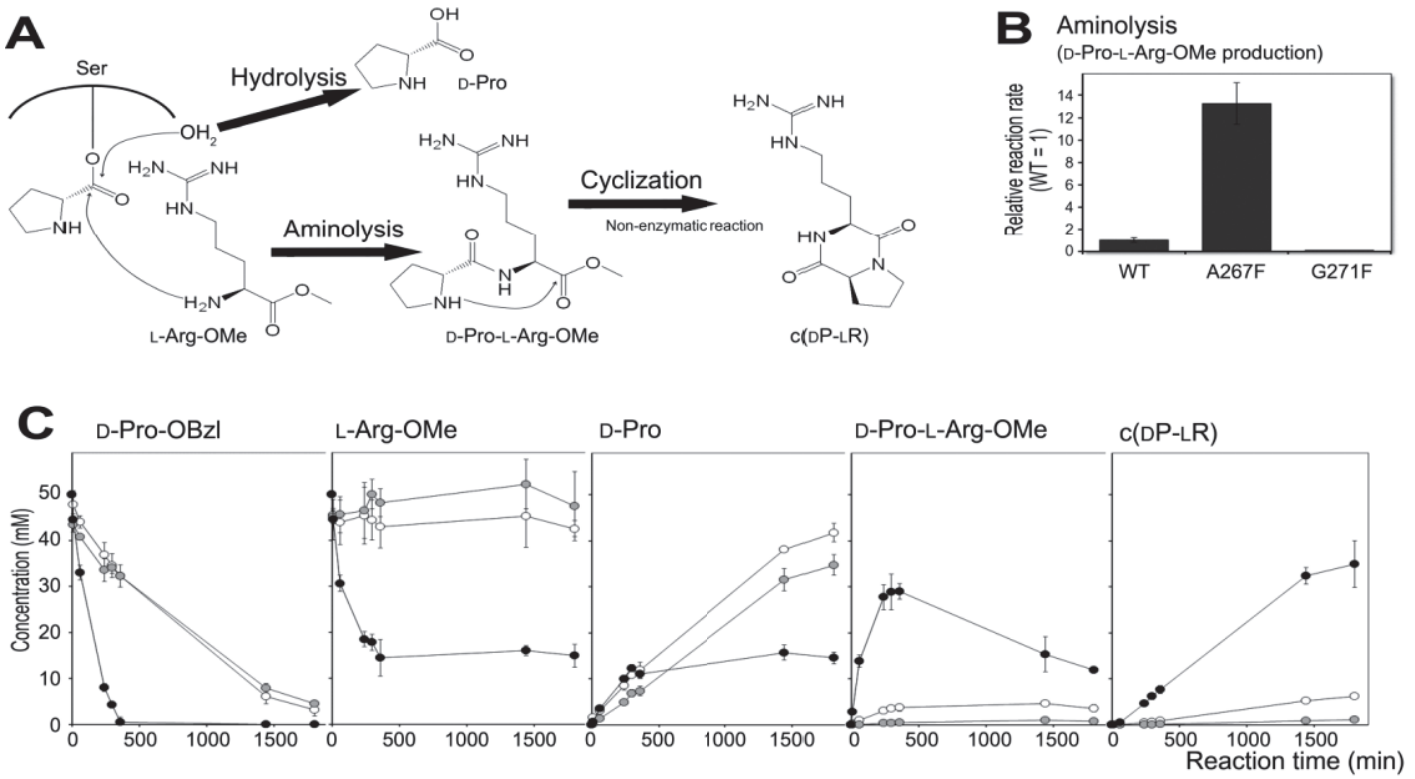

Fig. 4.5 Effect of mutation on c(DP-LR) synthesis by aminolysis function of DAH. (A) Reaction scheme of the DAH reaction for D-Pro-L-Arg-OMe. (B) Comparison of reaction rate for aminolysis among WT, A267F and G271 DAHs using D-Pro-OBzl and L-Arg-OMe as acyl donor and acceptor substrates, respectively. (C) Time dependence of c($_{D}$P-$_{L}$R) synthesis by aminolysis function of WT (*open circles*), A267F (*black circles*) and G271F (*gray circles*) DAHs. All panels indicate the profiles of the substrate concentration or product shown above the respective panels. The reaction was continued up to 30 h. The reactions were performed in solutions containing 50 mM substrates at pH 8.5 and 4 °C. Each value represents the mean ± SD of values from four independent experiments

4.4 DISCUSSION

In the structure of DAH, a small pocket exists in the vicinity of the active site Ser86 and is predicted to accommodate substrate(Arima et al. 2016). This structure is a common feature among serine peptidases belonging to family S12 in MEROPS. In fact, several of the enzymes of the S12 family exhibit high aminolysis activity(Kato et al. 1990; Komeda and Asano 1999; Matsushita-Morita et al. 2013), and five crystal structures of S12 family peptidases, including DAH (PDB: 3WWX), have been reported to date: D-stereospecific aminopeptidase (PDB: 1EI5), D, D-peptidase (PDB: 3PTE), class C β-lactamase (PDB: 1BLS), and D-amino acid amidase (PDB: 2EFX) (Lobkovskya et al. 1994; Kelly and Kuzin 1995; Bompard-Gilles et al. 2000; Okazaki et al. 2007). Among them, D-stereospecific aminopeptidase and D, D-peptidase as well as DAH, catalyze aminolysis reaction(Kato et al. 1990; Pratt and Frère 2013). As the common feature in the structure of the enzymes catalyzing aminolysis, they possess a large cavity that leads to the catalytic center. In contrast, the structure of D-amino acid amidase, which functions only hydrolysis catalysis, possess a narrow tunnel instead of the cavity (Okazaki et al. 2007). Because wide space of the cavity allows accessing of acyl acceptor substrate to the catalytic center, a large cavity is considered necessary to have the function of aminolysis. Meanwhile, Okazaki et al. reported that the structure of D-amino acid amidase pocket fits L-Phe and D-Phe (Okazaki et al. 2007, 2008a). In this structure, unlike the bound D-Phe that forms an acyl-enzyme intermediate, the bound L-Phe does not form an acyl-enzyme intermediate. Although D-amino acid amidase cannot catalyze aminolysis, the pocket shape and the arrangement of amino acid residues constituting the active site pocket of D-amino acid amidase were similar to those of DAH(Arima et al. 2016). As portrayed in Fig. 4.4 D, DAH strictly recognizes L-amino acids as

acyl acceptor substrate. Thus, the pocket presumably functions to recognize acyl acceptors for aminolysis in addition to the recognition of acyl donor substrate.

Our previous report presents the multiple functions of active site pocket in aminolysis and accompanying processes of the reaction; *i.e.*, substrate recognition, acyl-enzyme intermediate formation, and nucleophilicity of acyl acceptor substrate. The study revealed that the expansion of the space and the changes in local flexibility and the electrostatic environment of the active site pocket affected the aminolysis catalysis of DAH (Elyas et al. 2018). Although the enhancement of aminolysis activity by the expansion of the space of active site pocket was observed in several mutant DAHs, the mechanism on the catalytic functions of DAH including recognition of acyl donor and acceptor substrates in aminolysis reaction remained unresolved. Functional analysis of residues comprising the active site pocket by the different approach from the previous study should provide insights into the catalytic mechanism, including substrate recognition. In this study, we investigated the effect of space filling of active site pocket on aminolysis function of DAH with an assumption that a different effect from the expansion of the pocket would be observed.

The structure of the active site pocket of DAH dramatically changed by mutation; the pocket spaces in the predicted structures of A267F and G271F DAHs is narrower than that of WT (Fig. 4.3 B). Such drastic modifications of the pocket structure would be likely to significantly reduce catalytic ability. However, DAH retained its acyl-enzyme intermediate formation and hydrolysis function even after Ala267 and Gly271 were substituted with Phe (Fig. 4.4 B and 4.4 C). Additionally as shown in Fig. 4.4 D and 4.5 B, substitution of Ala267 to Phe resulted in enhance of aminolysis efficiency. In contrast, G271F DAH exhibited significantly lower aminolysis activity. Because the space filling of active site pocket dramatically affects

aminolysis function of DAH as described above, the active site pocket is clearly involved in the acyl acceptor preference for aminolysis reaction. Although the mutations of Ala267 and Gly271 to Phe led the space of active site pocket narrower than WT DAH (Fig. 4.3 B), the effects of both mutations on aminolysis activity were totally different from each other. Especially A267F DAH accepted L-Trp and L-Arg-OMe, of which the feature of the side chains are totally different from each other, as preferred acyl acceptor substrates (Fig. 4.4 D and 4.5B), suggesting that the shape and electrostatic environment of A267F DAH active site pocket is fit for nucleophilic attack by acyl acceptor substrate.

Although we could not conclude how the mutation of Ala267 to Phe affects the recognition mechanism of acyl acceptor substrate, this study revealed the effect of the space filling of active site pocket on aminolysis and led the construction of high-performance biocatalyst for c($_{D}$P-$_{L}$R) synthesis. Results of this study demonstrated that the aminolysis activity of A267F DAH superior to that of WT and mutant DAHs including the DAH variants constructed in our previous study. The mutant DAH might be able to solve the problems of undesired hydrolysis reaction in enzymatic aminolysis reaction for synthesis of biologically active substances. Next task of this study is to realize the synthesis of various biologically active peptides by using the mutant DAH constructed in this study.

4.5 CONCLUSION

In this study, we assessed the effect of the space filling of the active site pocket of DAH on its aminolysis activity by constructing two mutants A267F and G271F DAHs. By the investigation of the effect of space modification on the respective steps for hydrolysis and aminolysis catalysis, the mutation of Ala267 to Phe significantly enhanced the rate for condensation production by aminolysis reaction when L-Trp was used as acyl acceptor substrate whereas no enhancement

rather decreases in activity was observed by the mutation of Gly271 to Phe. A similar effect of mutation was observed in the efficiency of the synthetic activity of c($_{D}$P-$_{L}$R). Although we could not conclude how the mutation of Ala267 to Phe affects the recognition mechanism of acyl acceptor substrate, this mutant might be considered as a high-performance biocatalyst for biologically active dipeptides synthesis.

CHAPTER FIVE

SUMMARY FOR THE STUDY

Recently D-Stereospecific amidohydrolase (DAH) obtained from *Streptomyces* sp. 82F2 isolated from soil samples. The enzyme belongs to S12 family serine peptidase and categorized as D-Stereospecific peptidase. DAH exhibited high aminolysis reaction in accordance with hydrolysis. DAH recognizes D-amino acyl ester derivatives as substrates and catalyzes hydrolysis and aminolysis to yield D-amino acids and D-amino acyl peptides or amide derivatives, respectively. In the aminolysis, DAH preferentially utilizes D-amino acyl derivatives as acyl donor and L-amino acyl derivatives as acyl acceptor to synthesize dipeptides with DL-configuration.

Crystal structure of DAH that bind with 1,8-diaminooctane was resolved at resolution 1.49Å((PDB: 3WWX), the structural analysis has revealed that DAH possesses large cavity leads to catalytic center S86 which positioned at the center of the large cavity, close to the catalytic center of Ser86, lys89 and Tyr191 there is a small pocket at the bottom. Because the pocket is close to the catalytic center and is thought to interact with substrates during the catalytic reaction. Structural compersion of S12 family members and DAH revealed the overall structures of S12 enzyme family members are similar, although there are significant differences in terms of the shapes and sizes of the cavities and active site pockets among them. In DAH the enzyme has a large cavity and active site pocket. This large cavity in DAH allows the peptide substrate to enter, and the large space in the active site pocket accommodates the large side chain of the acyl donor substrate. DAH pocket composes of a number of hydrophobic residues these residues seem to involved in acyl donor and acyl acceptor during the catalytic reaction. the active

site pocket plays a functional role in substrate recognition, and the factors related to the hydrolysis, preference of acyl acceptor in the aminolysis reaction and stereoselectivity of the substrate are still unclear. Therefore, the present study was conducted to elucidate the function of the pocket in the catalytic activity of DAH. we investigated the role of residues constituting the active site pocket via mutational analysis, these investigations have illustrated the strong relationship between the pocket structure and catalytic activity such as acyl-enzyme intermediate formation, hydrolysis reaction, and aminolysis. overall results provide useful information insight into the mechanism of substrate recognition aiming to develop a convenient biocatalyst for peptide synthesis.

Chapter one outlines the aims of this dissertation, provides a literature review of the relative studies on serine protease and their structure and mechanism of the reaction, and also provides a brief background on the origin of DAH, crystal structure, mechanism of catalytic reaction and function of biologically active dipeptide synthesis by aminolysis reaction.

In Chapter two, we analyzed the function of the eight residues that form the pocket (Tyr144, Thr145, Phe150, Val154, Phe155, Ile266, Ile338, and His339) in terms of substrate recognition and aminolysis by mutational analysis. Formation of the acyl-enzyme intermediate and catalysis of aminolysis by DAH were changed by substitutions of selected residues with Ala. In particular, I338A DAH exhibited a significant increase in the condensation product of Ac-D-Phe methyl ester and 1,8-diaminooctane (Ac-D-Phe-1,8-diaminooctane) compared with the wild-type DAH. A similar effect was observed by the mutation of Ile338 to Gly and Ser. The pocket shapes and local flexibility of the mutants I338G, I338A, and I338S are thought to resemble each other. Thus, changes in the shape and local flexibility of the pocket of DAH by mutation presumably alter substrate recognition for aminolysis.

In chapter three, this study addresses the effects of modifying the active site pocket of DAH on the recognition of stereoselectivity and hydrophobicity of substrates and on the formation of enzyme-acyl intermediate. Structural comparison of DAH with substrate-bound D-amino acid, amidase revealed that three residues located in the active site pocket of DAH (Thr145, Ala267, and Gly271) might be involved in interactions with D-phenylalanine substrate. We substituted Ala267 and Gly271, which are located at the bottom of the hydrophobic pocket of DAH, with Phe and observed changes in the stereoselectivity and specific activity toward the free and acetylated forms of D/L-Phe-methyl esters. In contrast, the mutation of Thr145, which likely supplies a negative charge for recognition of the amino group of the substrate, hardly affected the stereoselectivity of the enzyme. Substrate binding by DAH was disrupted by the mutation of Ala267 to Val or Trp and kinetic analysis showed that the hydrophobicity of the bottom of the active site pocket (Ala267 and Gly271) is important for both stereoselectivity and recognizing hydrophobic substrates.

In Chapter four, this study aims to assess the effect of the space filling of the active site pocket of D-stereospecific amidohydrolase (DAH) on catalytic activity in order to enhance the aminolysis activity of the enzyme. Two mutants A267F and G271F DAHs were designed to fill the space of active site pocket of DAH. Then we investigated the effect of space modification on the acyl-enzyme intermediates formation, hydrolysis, and aminolysis catalysis. Methanol release from acetylated D-Phe methyl ester, which represents the acyl-enzyme intermediate formation, was observed to be higher in A267F by three-fold than that of WT. In addition, A267F DAH exhibited a significant increase in condensation production by aminolysis reaction when L-Trp was used as acyl acceptor substrate. In contrast to A267F DAH, no enhancement rather decrease in activity was observed by the mutation of Gly271 to Phe. A similar effect of mutation was

observed in the efficiency of the synthetic activity of chitinases inhibitor cyclic dipeptide, cyclo(D-Pro-L-Arg), the lead compound for the development of antifungal reagents and insecticides. A276F DAH showed high aminolysis activity and improved the reaction rate for cyclo(D-Pro-L-Arg) production. This mutant might be considered as a high-performance biocatalyst for biologically active dipeptides synthesis.

要旨

土壌放線菌 *Streptomyces* sp. 82F2 が生産する D 体特異的アミノ酸アミド加水分解酵素（DAH）は、S12 ファミリーのセリン型 D 体特異的ペプチダーゼに属する酵素である。DAH は、加水分解の副反応としてアミノリシス活性を示し、D-アミノ酸エステル誘導体をアシル受容体基質として、L-アミノ酸及びその誘導体をアシル受容体基質として認識するため、D-／L-配列を有するジペプチドを特異的に合成する。

DAH の立体構造解析（PDB: 3WWX）から、DAH は活性中心へと続く大きなくぼみの中に基質結合部位と思われるポケットが存在し、その側に活性中心 Ser86、Lys89、Tyr191 があることが明らかとなっている。DAH の全体構造は、S12 ファミリーに属する酵素と非常に類似したものであるが、このくぼみとポケットの構造は他の同属酵素と大きく異なり、DAH は他の酵素よりくぼみやポケットは大きいため、この構造が、よりペプチドや大きな側鎖を持つアミノ酸誘導体を基質として認識できることに起因していると考えられた。また、DAH のポケットを構成するアミノ酸残基の多くは疎水性であり、これらが酵素の基質認識に対し何らかの役割を果たすことも予想できる。しかし、それらの機能やメカニズムは明らかではない。そこで本研究ではこのポケット構造やポケットを構成するアミノ酸残基に焦点を当て、DAH のアシル酵素中間体形成や加水分解、アミノリシス活性などの変異による影響を調べ、ポケット構造と DAH 触媒活性との関連について検討した。本研究で得られた成果は、DAH をベースとしたジペプチド合成ツールとしての生体触媒の構築に大きく寄与するものであり、博士論文では、それらの具体的な内容と成果をまとめた。

第 2 章では、DAH のポケットを構築する 8 つの残基に変異を加え、それぞれのアミノリシスにおける基質認識における役割を検証し、ポケットの広さがアミノリシス活性に大きく影響することを述べている。本実験において、Ile338 を Ala に置換することで、Ac-D-Phe-OMe と 1,8-diaminooctane を基質としたときのアミノリシス活性が顕著な上昇が観察された。同様の効果は Ile338 を Gly や Ser に置換することでも観察されたことから、大きな側鎖を持つ Ile から小さな側鎖のアミノ酸への置換によるポケットの拡大と柔軟性向上が、アミノリシス活性の基質認識に影響を与えたと考えられた。

第 3 章では、DAH のポケット形状の改変における基質の立体選択性や疎水性基質への選択性に対する影響について述べている。DAH の立体構造と D-アミノ酸アミダーゼの構造比較から、DAH ポケットの底に存在する残基（Ala267、Gly271）が、基質としての D-Phe の認識に大きく関わっていると推定された。それぞれの残基の側鎖は小さいため、Phe に置換してスペースを埋め、Ac/H-D/L-Phe-OMe を基質とした反応の変化を観察することで検証した。その結果、Ala267 を Phe に置換すると、立体選択性が変化し、疎水基質に対する特異性が維持されたほか、一律に反応速度が向上した。一方で、Ala267 を Val や Trp、Gly271 を Phe に置換すると、Ac/H-D/L-Phe-OMe への認識が極端に低下したため、ポケットの底の形状や疎水環境が立体選択性や基質認識に大きく関わることが示唆された。

第 4 章では、上記検討によって得られた A267F が、非常に高いジペプチド合成活性を示すことが見出されたため、Ala267 の Phe への変異の優位性の立証について述べている。G271F DAH と野生型を比較対象とし、D-アミノ酸-OMe 及び L-アミノ酸を使用した

ジペプチド合成反応の第一段階である MeOH 遊離活性について検証した結果、G271F DAH は野生型の半分程度であったことに対し、A267F は野生型より 3 倍高い結果となった。しかし、いずれの酵素の加水分解活性は同程度であった。一方で生成ジペプチド量は A267F が顕著に高く、G271G は野生型より低い結果となった。同様の効果は、殺虫剤のリード化合物である cyclo(D-Pro-L-Arg)の合成においても観察された。以上の結果から、Ala267 の Phe への変異は本酵素のジペプチド合成活性に対し優位な効果が認められ、DAH をベースとした生理活性ジペプチド合成用高機能生体触媒の構築において、有用となる情報が得られた。

REFERENCES:

Allain CC, Poon LS, Chan CS, et al (1974) Enzymatic determination of total serum cholesterol. Clin Chem 20:470–475

Andrew D. Mesecar DEKJ (2000) A new model for protein stereospecificity T. Nature 403:614–615

Arima J, Chiba M, Ichiyanagi T, et al (2010a) Eryngase: *a Pleurotus eryngii* aminopeptidase exhibiting peptide bond formation activity. Appl Microbiol Biotechnol 87:1791–1801. doi: 10.1007/s00253-010-2663-7

Arima J, Ito H, Hatanaka T, Mori N (2011a) Aminolytic reaction catalyzed by d-stereospecific amidohydrolases from Streptomyces spp. Biochimie 93:1460–1469. doi: 10.1016/j.biochi.2011.04.020

Arima J, Morimoto M, Usuki H, et al (2010b) β-Alanyl peptide synthesis by Streptomyces S9 aminopeptidase. J Biotechnol 147:52–58. doi: 10.1016/J.JBIOTEC.2010.03.007

Arima J, Shimone K, Miyatani K, et al (2016) Crystal structure of d -stereospecific amidohydrolase from Streptomyces sp. 82F2 - Insight into the structural factors for substrate specificity. FEBS J 283:337–349. doi: 10.1111/febs.13579

Arima J, Tanaka A, Morimoto M, Mori N (2014) Mutation of active site serine residue with cysteine displays change in acyl-acceptor preference of β-peptidyl aminopeptidase from Pseudomonas aeruginosa PAO1. Appl Microbiol Biotechnol 98:1631–1640. doi: 10.1007/s00253-013-4992-9

Arima J, Usuki H, Hatanaka T, Mori N (2011b) One-pot synthesis of diverse DL-configuration dipeptides by a Streptomyces D-stereospecific amidohydrolase. Appl Environ Microbiol 77:8209–8218. doi: 10.1128/AEM.05543-11

Arnold K, Bordoli L, Kopp J, Schwede T (2006a) The SWISS-MODEL workspace: A web-based environment for protein structure homology modelling. Bioinformatics. doi: 10.1093/bioinformatics/bti770

Arnold K, Bordoli L, Kopp J, Schwede T (2006b) The SWISS-MODEL workspace: a web-based environment for protein structure homology modelling. Bioinformatics 22:195–201. doi: 10.1093/bioinformatics/bti770

Asano Y, Lübbehüsen TL (2000) Enzymes acting on peptides containing D-amino acid. J Biosci Bioeng 89:295–306

Asano Y, Nakazawa A, Kato Y, Kondo K (1989) Properties of a novel D-stereospecific aminopeptidase from Ochrobactrum anthropi. J Biol Chem 264:14233–9

Biasini M, Bienert S, Waterhouse A, et al (2014a) SWISS-MODEL: modelling protein tertiary and quaternary structure using evolutionary information. Nucleic Acids Res 42:W252–W258. doi: 10.1093/nar/gku340

Biasini M, Bienert S, Waterhouse A, et al (2014b) SWISS-MODEL: Modelling protein tertiary and quaternary structure using evolutionary information. Nucleic Acids Res 42:W252–W258. doi: 10.1093/nar/gku340

Bompard-Gilles C, Remaut H, Villeret V, et al (2000) Crystal structure of a D-aminopeptidase from Ochrobactrum anthropi, a new member of the “penicillin-recognizing enzyme” family. Structure 8:971–80

Bordusa F (2002) Proteases in Organic Synthesis. Chem Rev 102:4817−4867. doi: 10.1021/cr010164d

Bratovanova EK, Petkov DD (1987) Glycine flanked by hydrophobic bulky amino acid residues as minimal sequence for effective subtilisin catalysis. Biochem J 248:957–60

Craik C, Largman C, Fletcher T, et al (1985) Redesigning trypsin: alteration of substrate specificity. Science (80-) 228:291–297. doi: 10.1126/science.3838593

Delmarcelle M, Boursoit M-C, Filée P, et al (2005a) Specificity inversion of Ochrobactrum anthropi D-aminopeptidase to a D,D-carboxypeptidase with new penicillin binding activity by directed mutagenesis. Protein Sci 14:2296–2303. doi: 10.1110/ps.051475305

Delmarcelle ML, Boursoit M-C, Filé P, et al (2005b) Specificity inversion of Ochrobactrum anthropi D-aminopeptidase to a D,D-carboxypeptidase with new penicillin binding activity by directed mutagenesis. Protein Sci 14:2296–303. doi: 10.1110/ps.051475305

Dodson G, Wlodawer A (1998) Catalytic triads and their relatives. Trends Biochem Sci 23:347–52

Ekici ÖD, Paetzel M, Dalbey RE (2008) Unconventional serine proteases: Variations on the catalytic Ser/His/Asp triad configuration. Protein Sci 17:2023–2037. doi: 10.1110/ps.035436.108

Elyas YYA, Miyatani K, Bito T, et al (2018) Active site pocket of Streptomyces d -stereospecific amidohydrolase has functional roles in aminolysis activity. J Biosci Bioeng. doi: 10.1016/j.jbiosc.2018.03.004

Fields PA (2001) Review: Protein function at thermal extremes: balancing stability and flexibility. Comp Biochem Physiol Part A Mol Integr Physiol 129:417–431. doi: 10.1016/S1095-6433(00)00359-7

Goswami A, Van Lanen SG (2015) Enzymatic strategies and biocatalysts for amide bond formation: tricks of the trade outside of the ribosome. Mol BioSyst 11:338–353. doi: 10.1039/C4MB00627E

Heck T, Kohler H-PE, Limbach M, et al (2007) Enzyme-Catalyzed Formation ofβ-Peptides:β-Peptidyl Aminopeptidases BapA and DmpA Acting asβ-Peptide-Synthesizing Enzymes. Chem Biodivers 4:2016–2030. doi: 10.1002/cbdv.200790168

Hedstrom L (2002a) Serine Protease Mechanism and Specificity. Chem Rev 102:4501–4523. doi: 10.1021/CR000033X

Hedstrom L (2002b) Serine Protease Mechanism and Specificity. Chem Rev 102:4501−4523. doi: 10.1021/cr000033x

Houston DR, Eggleston IM, Synstad B, et al (2002) The cyclic dipeptide CI-4 [cyclo-(L-Arg-D-Pro)] inhibits family 18 chitinases by structural mimicry of a reaction intermediate. Biochem J 27:23–27

Houston DR, Synstad B, Eijsink VGH, et al (2004) Structure-based exploration of cyclic dipeptide chitinase inhibitors. J Med Chem 47:5713–5720. doi: 10.1021/jm049940a

Izumida H, Imamura N, Sano H (1996) A Novel Chitinase Inhibitor from a Marine Bacterium, Pseudomonas sp. J Antibiot (Tokyo) 49:76–80

John J. Perona and Charles S. Craik (1995) Structural basis of substrate specificity in the serine proteases. Protein Sci 4:337–360

Kato Y, Asano Y, Nakazawa A, Kondo K (1989) First stereoselective synthesis of D-amino acid N-alkyl amide catalyzed by D-aminopeptidase. Tetrahedron 45:5743–5754. doi: 10.1016/S0040-4020(01)89103-1

Kato Y, Asano Y, Nakazawa A, Kondo K (1990) Synthesis of D-Alanine Oligopeptides Catalyzed by D-Aminopeptidase in Non-Aqueous Media. Biocatal Biotransformation 3:207–215. doi: 10.3109/10242429008992063

Kelly JA, Kuzin AP (1995) The Refined Crystallographic Structure of aDD-Peptidase Penicillin-target Enzyme at 1.6 Å Resolution. J Mol Biol 254:223–236. doi: 10.1006/jmbi.1995.0613

Komeda H, Asano Y (1999) Synthesis of d-phenylalanine oligopeptides catalyzed by alkaline d-peptidase from Bacillus cereus DF4-B. J Mol Catal B Enzym 6:379–386. doi: 10.1016/S1381-1177(98)00136-2

Kumar I, Pratt RF (2005) Transpeptidation Reactions of a Specific Substrate Catalyzed by the Streptomyces R61 DD-Peptidase: Characterization of a Chromogenic Substrate and Acyl Acceptor Design †. 44:9971–9979. doi: 10.1021/bi050542z

Kyte J, Doolittle RF (1982) A Simple Method for Displaying the Hydropathic Character of a Protein. J Mol Biol 157:105–132

Laemmli UK (1970) Cleavage of structural proteins during the assembly of the head of bacteriophage T4. Nature 227:680–5. doi: 10.1038/227680A0

Lobkovskya E, Billings EM, Moews PC, et al (1994) Crystallographic Structure of a Phosphonate Derivative of the Enterobacter cloacae P99 Cephalosporinase: Mechanistic Interpretation of a /3-Lactamase Transition-State Analog. Biochemistry 33:6762–6772

López-otín C, Matrisian LM (2007) Emerging roles of proteases in tumor suppression. Nature 7:800–808

Mangos TJ, Haas MJ (1996) Enzymatic Determination of Methanol with Alcohol Oxidase, Peroxidase, and the Chromogen 2,2′-Azinobis(3-ethylbenzthiazoline-6-sulfonic acid) and Its Application to the Determination of the Methyl Ester Content of Pectins. JAgricFoodChem 44:2977–2981

Matsushita-Morita M, Nakagawa H, Tada S, et al (2013) Characterization of a D-stereoselective aminopeptidase (DamA) exhibiting aminolytic activity and halophilicity from aspergillus oryzae. Appl Biochem Biotechnol 171:145–164. doi: 10.1007/s12010-013-0330-z

Matthews DA, Alden RA, Birktoft JJ, et al (1977) Re-examination of the charge relay system in subtilisin comparison with other serine proteases. J Biol Chem 252:8875–83

Morrison KL, Weiss GA (2001) Combinatorial alanine-scanning. Curr Opin Chem Biol 5:302–7

Mótyán János András TF and TJ (2013) Research Applications of Proteolytic Enzymes in Molecular Biology. Biomolecules 3:923–942. doi: 10.3390/biom3040923

Okazaki S, Suzuki A, Komeda H, et al (2007) Crystal Structure and Functional Characterization of a D-Stereospecific Amino Acid Amidase from Ochrobactrum anthropi SV3, a New

Member of the Penicillin-recognizing Proteins. J Mol Biol 368:79–91. doi: 10.1016/j.jmb.2006.10.070

Okazaki S, Suzuki A, Mizushima T, et al (2008a) Structures of D -amino-acid amidase complexed with L -phenylalanine and with L -phenylalanine amide: insight into the D -stereospecificity of D -amino-acid amidase from *Ochrobactrum anthropi* SV3. Acta Crystallogr Sect D Biol Crystallogr 64:331–334. doi: 10.1107/S0907444907067479

Okazaki S, Suzuki A, Mizushima T, et al (2008b) Structures of D-amino-acid amidase complexed with L-phenylalanine and with L-phenylalanine amide: Insight into the D-stereospecificity of D-amino-acid amidase from Ochrobactrum anthropi SV3. Acta Crystallogr Sect D Biol Crystallogr 64:331–334. doi: 10.1107/S0907444907067479

Paetzel M, Dalbey RE (1997) Catalytic hydroxyl/amine dyads within serine proteases. Trends Biochem Sci 22:28–31. doi: 10.1016/S0968-0004(96)10065-7

Paetzel M, J. Strynadka NC (2008) Common protein architecture and binding sites in proteases utilizing a Ser/Lys dyad mechanism. Protein Sci 8:2533–2536. doi: 10.1110/ps.8.11.2533

Page MJ, Di Cera E (2008) Serine peptidases: Classification, structure and function. Cell Mol Life Sci 65:1220–1236. doi: 10.1007/s00018-008-7565-9

Pettersen EF, Goddard TD, Huang CC, et al (2004) UCSF Chimera-A visualization system for exploratory research and analysis. J Comput Chem 25:1605–1612. doi: 10.1002/jcc.20084

Polgár L (2005) The catalytic triad of serine peptidases. Cell Mol Life Sci 62:2161–2172. doi: 10.1007/s00018-005-5160-x

Polgár L, Bender ML (1969) The nature of general base-general acid catalysis in serine proteases. Proc Natl Acad Sci U S A 64:1335–42

Pratt RF, Frère J-M (2013) Streptomyces R61 d-Ala-d-Ala Carboxypeptidase. In: Handbook of Proteolytic Enzymes. Elsevier, pp 3458–3463

Rawlings ND (2016) Peptidase specificity from the substrate cleavage collection in the MEROPS database and a tool to measure cleavage site conservation. Biochimie 122:5–30. doi: 10.1016/j.biochi.2015.10.003

Rawlings ND (2009) A large and accurate collection of peptidase cleavages in the MEROPS database. Database. doi: 10.1093/database/bap015

Rawlings ND, Barrett AJ (1993) Evolutionary families of peptidases. Biochem J 290 (Pt 1):205–18

Rawlings ND, Barrett AJ (1994) Proteolytic Enzymes: Serine and Cysteine Peptidases

Rawlings ND, Barrett AJ, Finn R (2016) Twenty years of the *MEROPS* database of proteolytic enzymes, their substrates and inhibitors. Nucleic Acids Res 44:D343–D350. doi: 10.1093/nar/gkv1118

Rawlings ND, Barrett AJ, Thomas PD, et al (2018) The MEROPS database of proteolytic enzymes, their substrates and inhibitors in 2017 and a comparison with peptidases in the PANTHER database. Nucleic Acids Res 46:D624–D632. doi: 10.1093/nar/gkx1134

Sauvage E, Kerff F, Terrak M, et al (2008) The penicillin-binding proteins: structure and role in peptidoglycan biosynthesis. FEMS Microbiol Rev 32:234–258. doi: 10.1111/j.1574-6976.2008.00105.x

Shin S, Yun YS, Koo HM, et al (2003) Characterization of a Novel Ser- *cis* Ser-Lys Catalytic Triad in Comparison with the Classical Ser-His-Asp Triad. J Biol Chem 278:24937–24943. doi: 10.1074/jbc.M302156200

Tsai P-C, Fan Y, Kim J, et al (2010) Structural determinants for the stereoselective hydrolysis of chiral substrates by phosphotriesterase. Biochemistry 49:7988–97. doi: 10.1021/bi101058z

Wombacher R, Keiper S, Suhm S, et al (2006) Control of Stereoselectivity in an Enzymatic Reaction by Backdoor Access. Angew Chem Int Ed Engl April 3:2469–2472. doi: 10.1002/anie.200503280

Yazawa K, Numata K (2014) Recent Advances in Chemoenzymatic Peptide Syntheses. Molecules 19:13755–13774. doi: 10.3390/molecules190913755

Yokozeki K, Hara S (2005) A novel and efficient enzymatic method for the production of peptides from unprotected starting materials. J Biotechnol 115:211–20. doi: 10.1016/j.jbiotec.2004.07.017

Zakharova E, Horvath MP, Goldenberg DP (2009) Structure of a serine protease poised to resynthesize a peptide bond. Proc Natl Acad Sci 106:11034–11039

LIST OF PUBLICATIONS

1- Elyas Y., Y. A, Miyatani, K., Bito, T., Uraji, M., Hatanaka, T., and Shimizu K., and Arima, J. Active site pocket of *Streptomyces* D-stereospecific amidohydrolase has functional roles in aminolysis activity, J. Biosci. Bioeng., (2018), http://dx.doi.org/10.1016/j.jbiosc.2018.03.004

*This article is corresponding to chapter two of the thesis.

2- Elyas Y., Y. A, Miyatani, K., Shimizu K., and Arima J. Effect of Active site pocket structure modification of D-Stereospecific amidohydrolase on the recognition of stereospecific and hydrophobic substrates, Mol Biotechnol (2018). https://doi.org/10.1007/s12033-018-0104-5.

*This article is corresponding to chapter three of the thesis.